

1 **The marked diversity of unique cortical enhancers enables**
2 **the generation of neuron-specific tools by Enhancer-Driven**
3 **Gene Expression (EDGE)**

4 Authors: Stefan Blankvoort¹, Menno Witter¹, James Noonan^{2,3}, Justin Cotney^{2,4,*}, Cliff Kentros^{1,5,*}

5

6

7 Author affiliations

8 1. Kavli Institute for Systems Neuroscience and Centre for Neural Computation, NTNU, Norway;

9 2. Department of Genetics, Yale School of Medicine, New Haven, CT, USA;

10 3. Kavli Institute for Neuroscience, Yale University, New Haven, CT, USA;

11 4. Department of Genetics and Genome Sciences, University of Connecticut Health Centre,
12 Farmington, CT, USA;

13 5. Institute of Neuroscience, University of Oregon, Eugene, OR, USA

14 * Corresponding authors: clifford.kentros@ntnu.no and cotney@uchc.edu

15 **SUMMARY**

16 Understanding neural circuit function requires individually addressing their component parts: specific
17 neuronal cell types. However, the precise genetic mechanisms specifying neuronal cell types remain
18 obscure. While most genes are expressed in the brain, the vast majority are expressed in many different
19 kinds of neurons, suggesting that promoters are not sufficiently specific to distinguish cell types. We
20 therefore examined distal genetic cis-regulatory elements controlling transcription (i.e. enhancers) in
21 closely related mouse cortical subregions. We identified thousands of novel putative enhancers, many
22 unique to particular cortical subregions. Remarkably, following pronuclear injection of constructs
23 containing such enhancers, we obtained transgenic lines driving expression in distinct sets of cells
24 specifically in the targeted cortical subregions. This not only helps illuminate the genetic mechanisms
25 underlying the specification of diverse neuronal cell types, it provides a general strategy for the
26 development of genetic tools targeting any neuronal circuit of interest via Enhancer-Driven Gene
27 Expression (EDGE).

28 INTRODUCTION

29 The mammalian brain is arguably the most complex biological structure known, composed of around
30 10^{11} neurons in humans[1]. While this number is generally accepted, the same is not true for how many
31 different *kinds* of neurons exist. Indeed, there is not even a clear consensus as to how to define a
32 neuronal cell type: by morphology, connectivity, gene expression, receptive field type, or some
33 combination of the above? If one takes the expansive view (i.e. all of the above), the numbers quickly
34 become astronomical. For example, current estimates of retinal cell types are between 100 and 150[2],
35 and dozens of cell types have been proposed for a single hypothalamic area based solely on which genes
36 are expressed[3]. Gene expression alone is a poor basis for defining cell types, however, because
37 although most genes are expressed in the adult brain, the vast majority of them are expressed in many
38 different cell types[4]. Identification of neuronal cell types is much more than an issue of taxonomy, it
39 is crucial to understanding brain function. The past two decades have seen the development of
40 revolutionary molecular tools which allow one to determine the precise connectivity of neurons[5, 6] as
41 well as manipulate[7-9] and observe[10] their activity. However, the utility of these powerful tools is
42 currently limited by the inability to deliver them at the level of particular neuronal cell types. Almost all
43 existing neuron-specific lines are either made by non-homologous recombination of minimal promoter
44 constructs[5, 11, 12] or knocking the transgene into the native transcript[13, 14]. Both of these
45 techniques depend upon the specificity of a native promoter, which as noted above is not specific
46 enough: one can recapitulate the expression of the native gene, but that gene will be expressed in
47 multiple neuronal cell types[15-17].

48 However, there must be *some* genetic basis for neuronal diversity. Investigations of transcriptional
49 regulation have revealed that spatiotemporally precise gene expression is achieved by the modular and
50 combinatorial action of a variety of trans-acting factors (i.e. DNA-binding proteins) interacting with
51 distinct cis-regulatory elements, regions of noncoding DNA termed enhancers[18]. While the exact
52 number of enhancers remains obscure, estimates run into the millions[19, 20], many times the number
53 of genes or promoters. This means that the same gene is presumably expressed in distinct cell types via

54 the activation of different sets of enhancers. Enhancers may therefore enable the generation of
55 molecular genetic tools more specific than possible using promoter-based methods. Indeed, many of
56 the most specific neuronal driver lines are likely the result of random integration next to a highly specific
57 enhancer[12, 21]. Fortunately, investigators studying the mechanisms of transcription have developed
58 a variety of techniques enabling the identification of the enhancers active in any tissue sample[22-26].
59 We reasoned that because different cell types are found in different brain regions, identifying enhancers
60 active only in particular brain regions could lead to region- and/or cell type-specific molecular genetic
61 tools, an approach that we call Enhancer Driven Gene Expression or EDGE (Figure 1).

62 RESULTS

63 Enhancer ChIP seq of cortical subregions reveals a striking diversity of unique 64 enhancers

65 Because promoter based techniques generally lead to gene expression throughout the telencephalon,
66 we specifically targeted closely related subregions of cortex in the hopes of obtaining regionally specific
67 tools. The following brain regions from two adult (P56) male C57BL6J mice were microdissected (for
68 details see methods and sup. Figure 1): the medial entorhinal cortex (MEC), the lateral entorhinal cortex
69 (LEC), the retrosplenial cortex (RSC), and the anterior cingulate cortex (ACC). Each mouse was processed
70 separately and the samples were used as biological replicates for further analysis. We performed ChIP-
71 seq on homogenized tissue against the active-enhancer-associated histone modifications H3K27ac and
72 H3K4me2 for samples of each of the four brain regions. The regions enriched for H3K27ac reproducibly
73 identified similar numbers of active promoters and distal cis-regulatory sequences between two
74 replicates of each brain subregion (Figure 2A). Nearly 90% of all active promoters were identified in at
75 least two samples with the remainder being active in only one subregion (17032 total, 2045 unique).

76 When we analyzed more distal sites (>5kb from a transcriptional start site) we identified a total of 59372
77 reproducibly active enhancers in at least one subregion. Of these 31% were only identified in a single
78 cortical subregion (18185 unique relative to other subregions). Surprisingly the number of subregion
79 specific enhancers in the cortex was similar to the number of total enhancers active in any single tissue
80 thus far interrogated[20, 27]. Furthermore 81% (48077) of enhancers identified in these subregions
81 were not identified in bulk cortex tissue from mouse demonstrating the potentially vast repertoire of
82 enhancers active in the brain.

83 Interestingly, when comparing the total number of reproducible peak calls in these 4 cortical subregions
84 (59372) to the number identified in bulk cortex treated in the same way (13472), the number of putative
85 active enhancers one obtains from the four cortical subregions is far greater than what one obtains from
86 the entire cortex, even though these four cortical regions compose only a small minority of the entire
87 cortex. Of course, this is comparing 4 pooled samples to a single sample, but each of the individual

88 samples gives numbers similar to bulk cortex (Figure 2). In our view the most likely explanation for this
89 superficially puzzling result is a reduction in signal to noise ratio when pooling heterogeneous sets of
90 tissues for ChIP-seq. This would tend to favor those enhancers that are expressed throughout many
91 cortical subregions at the expense of more specific ones. In support of this 89% of cortical enhancers
92 were found in one or more cortical subregions, and 78% were found in at least 2 cortical subregions.
93 Compare this to the fact that fully 31% of the enhancers we found in our subregions were specific to
94 that single subregion.

95 While many of these enhancers identified by peak calls alone are specific to this small number of cortical
96 subregions the goal of this study was to identify very specific regulatory sequences with limited activity
97 within other regions of the brain as well as the rest of the body. To ensure the identification of such
98 sequences and exclude regions with weak activity elsewhere we expanded our comparisons to include
99 a variety of published mouse adult tissues and cultured cell types[27]. We first identified active putative
100 enhancers in these additional mouse samples and merged them to create a unified set of enhancers for
101 consistent comparisons across all samples. We then extracted normalized H3K27ac counts at 108299
102 discrete regions from the subregions profiled in this study as well as those from 17 mouse ENCODE
103 samples[27]. Hierarchical clustering of samples revealed two main groups of mouse tissues: neuronal
104 and non-neuronal (Figure 2B). Amongst non-neuronal tissues, strongest correlations were observed
105 amongst developmental stages of heart and tissues that make up the immune system: bone marrow,
106 thymus, and spleen. In neuronal tissues the four cortical subregions profiled here were well correlated
107 across all enhancers assayed but clustered distinctly from cerebellum, olfactory bulb, and embryonic
108 brain.

109 We then utilized k-means clustering to identify enhancers that were significantly more active in each
110 cortical region versus each other (Figure 2C) and the other 17 mouse tissues. Those enhancers that
111 were identified as most specifically active in a given cortical sub-region were then further filtered to
112 ensure that they were never identified by peak calling in any other mouse tissue. This stringent analysis

113 yielded 165 to 1824 novel and unique putative distal enhancers for each cortical sub-region (Figure 2C,
114 sup. table 1). We then assigned these novel enhancers to putative target genes based upon the GREAT
115 algorithm[28]. Gene ontology analysis suggest these novel enhancers are enriched near genes
116 associated with a variety of neuronal functions (sup. Figure 2). We prioritized these novel putative
117 enhancers based on specificity of the H3K27ac signal relative to other regions and conservation across
118 30 species. We then cloned a subset of them specific to the entorhinal cortices (EC) upstream of a
119 heterologous minimal promoter driving the tetracycline transactivator (tTA[29]) for transgenesis (sup.
120 Figure 3).

121 **Region-specific enhancers drive transgene expression in the targeted cortical** 122 **subregions**

123 Of course, just because a sequence is identified by ChIP-seq does not mean that it is a valid enhancer,
124 let alone that it can drive region- or cell type-specific transgene expression. Even a single case of
125 expression in a particular tissue type is not sufficient because one can obtain specific transgene
126 expression by randomly inserting a minimal promoter/reporter construct into the genome. This
127 technique is known as an “enhancer trap” because it relies upon random insertion near a native
128 enhancer to drive the transgene expression[12, 30]. To ensure that the expression pattern comes from
129 the enhancer construct and not from the insertion site, the standard way to validate a putative enhancer
130 is to show that at least three distinct transgenic embryos (with three distinct random insertion sites)
131 have similar expression patterns[26]. We therefore injected enough oocytes to get at least three
132 genotypically-positive founders for each putative enhancer construct. However, since our aim was to
133 generate modular genetic tools rather than simply to validate the enhancers, we could not sacrifice the
134 founders to validate the enhancer as is typically done. Instead, the founders were crossed to tTA
135 dependent reporter mice for visualization of expression patterns.

136 We selected 8 (notionally) MEC-specific and 2 LEC-specific enhancers for transgenesis. Transgenesis via
137 pronuclear injection is not an extremely efficient process because it involves random integration into
138 the genome. While one typically only publishes the ones that work, we provide some detail about the

139 ones that did not because we are attempting to describe a method of transgenesis. Some founders do
140 not successfully transmit the transgene to offspring, while others fail to express presumably due to
141 negative insertional (a.k.a. positional) effects as opposed to the positive effects underlying an enhancer
142 trap[12, 30]. For these reasons, only 45 lines derived from 105 genotypically-positive founders
143 expressed in the brain when mated to a tetO reporter line. Notably, nearly all of them (41) expressed
144 the reporter in the EC, including at least one from each of the 10 enhancer constructs (sup. Figure 4 and
145 5, sup. Table 2). Since an enhancer trap would lead to random expression patterns, this alone suggests
146 that the specificity of expression comes from the transgenic enhancer. At least as compelling is the fact
147 that when we obtained multiple distinct founders with a given enhancer construct, almost all of them
148 had similar expression patterns (see sup. Figure 6 for examples).

149 Figure 3A shows an example of the results of our bioinformatic analysis for one of the eight MEC
150 enhancers (MEC-13-81, see methods for nomenclature) which GREAT associated with the gene *Kitl*.
151 Note that the promoter region (vertical yellow band) is a strong peak in all brain regions, consistent with
152 expression of the *Kitl* mRNA throughout the brain (Figure 3B). The same is true for other putative
153 enhancers (horizontal black bars). In contrast, the downstream enhancer peak used for transgenesis
154 (MEC-13-81, Figure 3A blow-up), while not as strong as some of the other peak calls, is greatly enriched
155 in MEC. Figure 3C shows the result of crossing the transgenic line MEC-13-81B to an tetO-ArchT payload
156 line[31]. Remarkably, even though the *Kitl* promoter expresses throughout the brain (including multiple
157 layers of the EC, Figure 3B), the tetO-ArchT payload is confined to layer II of MEC (Figure 3C). In other
158 words, one can obtain highly specific targeted gene expression from regionally specific cis-elements of
159 non-specific genes.

160 The same basic result of highly specific expression from single enhancers of non-specific genes was also
161 true for 4/8 MEC- and 2/2 LEC-specific enhancer constructs we injected. Figure 4 compares the
162 expression patterns of representative transgenic driver lines made with other injection constructs
163 containing either MEC-specific enhancers (Figure 4A to 4C, right column) or LEC-specific enhancers

164 (Figure 4D and E, right panel. Extended medial-lateral of sections range in sup. Figure 4) compared to
165 the expression pattern of the presumed associated native gene (Figure 4 left column). Note that while
166 the mRNA associated with each promoter is broadly expressed in the brain, the transgenic lines all
167 express more or less specifically in the brain region the enhancers were isolated from. These data show
168 that one can obtain targeted region-specific (and possibly even cell type-specific) expression from
169 elements of a non-specific promoter by using one of its region-specific enhancer to drive a heterologous
170 core promoter. Indeed, even those enhancers that were less specific still gave rise to lines that were
171 enriched in the EC relative to the expression of the native gene (sup. Figure 5). This in effect solves the
172 problem that most genes are expressed in multiple cell types in the brain: using EDGE one can dissect
173 out the individual genetic components underlying the expression of a gene in multiple cell types.

174 **Region versus cell type-specific expression?**

175 The above results show that one can get sub-region specific expression from sub-region specific
176 enhancers. Whether such enhancers drive expression in specific cell types in the targeted brain region
177 is a more difficult question to answer, in large part because there is no consensus as to the number of
178 cell types in the brain or even how to classify them. However, there are indications that some these
179 enhancers can specify particular cell types. First, the different EC enhancers tend to drive expression in
180 different layers of the EC (Figure 3 and 4), and neurons in different cortical layers are almost by definition
181 different cell types. By the same logic, some of these enhancers are clearly not cell type-specific (sup
182 Figure 5). Since three of the enhancers drive expression in layer II, this raises the question of whether
183 they specify the same cell type. We therefore investigated the expression of immunohistochemical
184 markers used to characterize cell types of EC in two layer II expressing lines derived from MEC-specific
185 enhancers (Figures 5A, B and 6A, B). The underlying logic is if the two distinct enhancers drive transgene
186 expression in subsets of the exact same cell type(s), they should both express the same proportions of
187 neurochemical markers. Neither of the two enhancers appear to drive expression in inhibitory neurons
188 (Figure 5I-L and 6I-L), so the question becomes whether they express in different types of excitatory
189 neurons. Excitatory neurons in EC layer II are typically further subdivided into reelin positive stellate

190 cells and calbindin positive pyramidal cells[32]. Line MEC-13-53A expressed exclusively in reelin+
191 neurons (Figure 5C-H, L), while line MEC-13-104B roughly corresponds to the relative densities of the
192 two celltypes (Figure 6C-H, L). Thus it appears that MEC-13-53A is a stellate cell specific enhancer,
193 whereas MEC-13-104B is found in both neurochemical kinds of excitatory cells of layer II described to
194 date. This means that some distinct enhancers can specify different subsets of cells even within a single
195 cortical layer, showing the potential of enhancers to distinguish between cell types with a finer
196 granularity than possible by promoters.

197 DISCUSSION

198 We demonstrate the existence of thousands of previously undescribed novel putative enhancers
199 uniquely active in targeted cortical subregions of the adult mouse brain. We took a small subset
200 (10/3740) of the enhancers so identified that were specific to the EC and combined them with a
201 heterologous minimal promoter to make transgenic mice expressing the tTA transactivator. When
202 crossed to tetO payload lines, we obtained transgene expression specific to the EC, and possibly even
203 particular cell types. This is true even though the genes that these enhancers presumably act upon are
204 not themselves specific. This suggests that there may be a genetic diversity in the brain beyond most
205 estimates of the number of distinct neuronal cell types in the cortex[33-36]. Moreover, it also provides
206 a strategy to make genetic tools with far greater cell type and regional specificity of expression than
207 promoter-based methods, by far the dominant means to generate neuron specific transgenic animals
208 to date (pronuclear injection of minimal promoters or BAC's, as well as knock-ins to native promoters
209 and/or gene-editing via CRISPR-Cas). This is because most genes (i.e. promoters) express in multiple cell
210 types in the brain. Since there are only around 24.000 genes (and around 46.000 promoters[19]), but
211 estimated millions of putative enhancers, this implies that the same gene is expressed in different cell
212 types by using different sets of enhancers acting upon the same promoter.

213 **EDGE is a method to create neuron-specific tools for targeted brain regions**

214 While the above discussion illustrates the power of this technique, it is important to be clear about what
215 is and is not novel about what has been presented here. A variety of forms of enhancer ChIP-seq have
216 existed for roughly a decade[22, 26], and the general concept that the same gene is expressed in
217 different tissues by the use of different enhancers is even older[30]. Hundreds of thousands of putative
218 enhancers have already been identified in the mouse genome by dissection of distinct tissues (including
219 cortex) followed by ChIP-seq[20, 27]. Indeed, a molecular geneticist in the transcription field may find
220 the results presented here unsurprising, as generation of a transgenic animal is how putative enhancers
221 are biologically verified, although the transgenic founders are typically killed in the process[22, 25, 26,

222 37]. In short, we have not created any novel techniques, but we demonstrate how the application of
223 these existing technologies to the adult brain can potentially revolutionize systems neuroscience by
224 providing a means to make cell type-specific tools in any brain region of interest.

225 There are many indications in the literature that this approach should work. A variety of recent papers
226 have used various techniques to suggest a highly diverse chromatin landscape in the adult brain,
227 indicative of a richness of enhancers. One group has performed ChIP-seq on 136 different dissected
228 human brain regions, obtaining over 80,000 putative enhancers[38]. Another group has used ATAC-seq
229 to profile open chromatin in transgenically-defined excitatory cells from different layers of the mouse
230 visual cortex[39]. They found a diversity of putative cis-acting sequences even within a single layer of a
231 single type of cortex, implying distinct classes of cells. Finally, using single cell methylomes, Luo et al.
232 have shown that neuron type classification is supported by the epigenomic state of regulatory
233 sequences[40]. However, in none of these cases were these putative enhancers biologically verified, nor
234 used to make molecular genetic tools, which is the point of this paper.

235 Conversely, many enhancers derived from the developing brain have in fact been biologically verified,
236 and even used to make transgenic lines and viruses[41]. Evolutionarily conserved single enhancers
237 demonstrably label specific subsets of cells during development[25, 26, 37, 42], with different subsets
238 active in different developmental epochs[43]. Of particular interest is a pair of papers from the
239 Rubenstein lab examining the activity of enhancers derived from the developing (E11.5) telencephalon.
240 They made CreER lines from the pallium (14 lines[44]) and subpallium (10 lines[45]) to illustrate the
241 fatemaps of the telencephalic subdivisions by comparing expression patterns at several timepoints
242 during development and young adulthood. Several of the enhancers expressed in specific subdivisions
243 of the developing telencephalon while others were more broadly expressed. By applying tamoxifen at
244 different developmental timepoints, they were able to elucidate distinct cell lineages in the
245 telencephalon. By examining in vivo transcription factor occupancy they showed that broadly expressed
246 transcription factors interact with far more specific enhancer elements[44].

247 Taken together, these studies clearly provide a large part of the underlying intellectual basis for what is
248 presented here. However, their focus is on the transcriptional and developmental mechanisms of neural
249 cell fate relatively early in development. As these and other studies demonstrate, every neuroepithelial
250 cell present at this time will have many[46, 47] daughter cells which will further differentiate during
251 development into many more neuronal, and indeed non-neuronal cell types. For this reason, these
252 enhancers show relatively broad expression in the adult brain[45], typically in neurons but sometimes
253 in endothelial cells (choroid plexus) in many different regions of the adult telencephalon. Subpallial
254 enhancers as expected tended to drive expression in GABAergic cells[41, 48], but do not distinguish
255 between the various known subtypes of GABAergic interneurons. For this reason although these tools
256 are valuable for elucidating cell lineages, they are not necessarily more specific than promoter-based
257 transgenic lines[15], which as noted earlier are not specific enough for the analysis of native neural
258 circuits.

259 Thus a seemingly trivial difference in technique results in a large increase in utility for systems
260 neuroscience. Applying the same methods discussed above to microdissected adult cortical subregions
261 allows one to make molecular genetic tools apparently specific to particular cell types of the targeted
262 brain regions. The microdissection is not a trivial feature: by examining four subregions of the cortex
263 separately, we found around four times as many reproducible peak calls as was obtained from the entire
264 cortex[27], even though these four subregions together comprise a small minority of the cortex. This
265 implies that individual cortical subregions contain their own epigenetically distinct cell types, which are
266 washed out when pooled. Similarly, there is in fact relatively little overlap between the enhancers active
267 in embryonic brain and those we have obtained from adult brain (Figure 2). Indeed, it would be
268 extremely interesting to work backwards and study the developmental expression of EDGE lines made
269 from subdivisions of the adult brain to investigate the genetic signatures of the pre- and postnatal
270 processes that specify the enormous variety of neuronal cell types present in the fully differentiated
271 adult brain. In sum, we do not claim to have discovered anything terribly novel about transcription in
272 the brain, although the sheer number of novel putative enhancers unique to cortical subregions was

273 indeed surprising. We also do not claim to have invented the methods described herein, they have
274 existed in the transcription field for the better part of the last decade. What we claim is both novel and
275 significant is the application of these methods to the generation of anatomically-specific tools enabling
276 the study of the circuit dynamics of the adult brain[49], rather than towards the study of transcriptional
277 control per se. Others have noted the promise of enhancers for the generation of neuron-specific tools,
278 these data demonstrate that promise is very real, and how one can do it for any brain region.

279 Understanding the brain at the circuit level requires the ability to deploy molecular tools at the level of
280 granularity at which native neural circuits operate. However, the promoter-based methods traditionally
281 used to express transgenes almost always fall short of this goal. The very infrequent exceptions are
282 either tools targeting the tiny minority of cell types associated with a single gene product or those few
283 instances where pronuclear injection of a minimal promoter construct leads to specificity far greater
284 than that of the original promoter by serendipitous insertional effects[21]. This latter phenomenon is in
285 essence an inadvertent enhancer trap strategy, which EDGE is basically the converse of. In enhancer
286 traps[12, 30], one randomly inserts a minimal promoter construct into the genome in the hopes of
287 integrating near a specific enhancer while EDGE involves the identification and use of enhancers specific
288 to particular brain regions. The key advantage of EDGE over enhancer traps is anatomical targeting. To
289 illustrate, we can compare our results to those of a recently published enhancer trap study[12] using a
290 lentiviral vector containing the exact same minimal promoter we used. Since we are interested in the
291 EC, we consider the creation of EC specific lines the goal, as in the current study. The total number of
292 genotypically positive founders that express in the brain are similar (45/105: 43% herein vs. 42/151:
293 28%), and both techniques can yield very specific expression patterns. The key difference is the numbers
294 of lines expressing in the EC at all (41/45: 91% herein vs. 6/42: 14%) and especially those more or less
295 specifically expressing in the EC (16/45: 36% vs. 0/42: 0%). This neatly shows the difference between
296 the two approaches: enhancer traps result in expression in random cell types throughout the brain (and
297 indeed the entire body), while EDGE targets those cell types found in particular brain regions of interest.

298 Of course not everyone is interested in the entorhinal cortex. Other investigators interested in other
299 brain regions can subtract out the brain regions *we* are interested in to develop tools specifically
300 targeting *their* brain regions of interest. This process can occur for any and all brain regions, potentially
301 providing cell type-specific tools to interrogate any neural circuit. Moreover, the more subdivisions of
302 the brain one collects, the more one can subtract, so therefore the more specific the resulting putative
303 enhancers will be. With this in mind we have initiated a second round of enhancer ChIP-seq with over
304 20 brain subregions which will provide a much more generally useful resource to the neuroscience
305 community at large than that which we have shared now. Finally, the relatively small size of these EDGE
306 hybrid promoters means they can fit easily in viral vectors. If EDGE viruses recapitulate the anatomical
307 specificity seen in transgenic mice, this will potentially bring the power of EDGE to bear on any
308 species[41]. This could revolutionize not only systems neuroscience, but ultimately provide a novel
309 therapeutic avenue to rectify the circuit imbalances that underlie disorders of the CNS.

310 **Do enhancers specify neuronal cell types in the brain?**

311 One of the most interesting questions in neuroscience is how we should think about the 100 or so billion
312 neurons in our brains- as unique actors, or as repeated elements in a printed circuit? Obviously the
313 answer is somewhere in between. Several investigators have proposed a canonical circuit for the
314 neocortex[50, 51] and there are clearly commonalities in neocortical circuits, particularly with regard to
315 layer specific connectivity. However, within this general canonical theme there are uniquely specialized
316 cell types in individual cortical subregions. Our results demonstrate that there are thousands of putative
317 enhancers unique to cortical subregions, a number that dwarfs the number of genes that are specific to
318 these subregions (indeed to our knowledge there are no EC specific genes). Why do the same genes use
319 different enhancers to express in different cortical subregions? We certainly do not have the answer,
320 but the developmental literature discussed above would suggest a combinatorial code of transcription
321 factors and active enhancers for each unique cell fate. If so, enhancer usage would provide a finer
322 grained differentiation of cell type than gene expression alone. The fact that there are hundreds to
323 thousands of unique enhancers in individual cortical subregions, implies that the genetic machinery

324 exists to have a similar number of differentiable cell types. In support of this, a recent study of the
325 transcriptome of thousands of individually sequenced neurons from two different cortical regions finds
326 a large number of distinct transcriptional profiles between excitatory, but not inhibitory neurons[52].
327 This (as well as the fact that inhibitory neurons are a small minority of cortical neurons) may explain why
328 we only obtained expression in excitatory neurons when we selected region-specific enhancers.

329 EDGE allows the generation of tools that provide a means to investigate the nature of neuronal cell
330 types. For example, three of the enhancer constructs presented here drive expression in layer II of MEC,
331 two of which (MEC-13-53 and MEC-13-81) exclusively in reelin-positive neurons (Figure 5 and data not
332 shown for MEC-13-81). MEC LII reelin-positive neurons are stellate cells, which is arguably a cell type,
333 but neither line expresses in 100% of reelin-positive neurons. There are two possible explanations of
334 this: the biologically interesting possibility is that these distinct enhancers drive expression in
335 functionally distinct subsets of stellate cells[52, 53]. The other, less interesting possibility is that each
336 enhancer drives expression in stellate cells as part of a co-regulated network of enhancers specifying
337 this cell type[38]. If so, the difference in percentage of expression in stellate cells is largely artefactual,
338 resulting from differential penetrance of transgene expression of otherwise identical cells due to
339 mosaicism arising from insertional effects. The exhaustive biochemical, anatomical and
340 electrophysiological characterization of each line necessary to provide a definitive answer to the
341 relationship between these enhancers and cell types is beyond the scope of this paper. However, the
342 fact that there are so many unique enhancers unique to specific cortical subregions implies that the
343 genetic potential exists for many more cell types than previously believed. Moreover, it is entirely
344 possible that further subdivisions of the cells specified by these transgenic lines could provide even
345 more specific expression. This could be achieved in a variety of ways, for example by finer manual
346 microdissection, laser capture microscopy or even nested ChIP-seq of transgenically-labeled cells
347 isolated by a cell sorter from microdissected tissue.

348 Regardless, we certainly do not mean to say that every enhancer defines a distinct cell type. Indeed
349 several of our lines express in more than one layer. There is not necessarily a one-to-one
350 correspondence between cell types and enhancers: a single cell type could be specified by multiple
351 unique enhancers, i.e. a co-regulated enhancer network[38]. Conversely, different cell types may arise
352 from distinct combinatorial codes of active enhancers, meaning the number of different cell types may
353 conceivably be even larger than the number of unique enhancers. Finally, there are other reasons for
354 differential sets of active enhancers beyond definition of cell type: neural activity in fact demonstrably
355 changes the chromatin landscape[54]. This suggests that the activity of differential enhancers does not
356 automatically imply different cell types but changes in function of a given cell. Nevertheless, differential
357 enhancer utilization does signify distinct genetic signatures, even if their functional significance is
358 currently unclear. We therefore maintain that the only way to properly investigate the relationship of
359 diverse cis-acting elements of the genome to the functional circuitry of the brain is to create and study
360 enhancer-specific tools like those presented herein.

361 **Author contribution**

362 Conceptualization: J.C. and C.K.

363 Methodology: S.B. and J.C.

364 Software: J.C.

365 Validation: S.B.

366 Formal analysis: J.C. and S.B.

367 Investigation: S.B., M.P.W. and J.C.

368 Resources: S.B., M.P.W. and J.C.

369 Data curation: S.B. and J.C.

370 Writing – original draft: S.B., J.C. and C.K.

371 Writing – review and editing: S.B., M.P.W., J.C. and C.K.,

372 Visualization: S.B. and J.C.

373 Supervision: J.C., J.N. and C.K.

374 Project administration: J.N. and C.K.

375 Funding acquisition: C.K.

376 **Acknowledgements**

377 We would like to acknowledge Haiyan Wu and Qiangwei Zhang for their help with *In Situ hybridization* ,

378 and Ute Hostick for her help with pronuclear injection.

- 379 1. von Bartheld CS, Bahney J, Herculano-Houzel S. The search for true numbers of neurons and
380 glial cells in the human brain: A review of 150 years of cell counting. *The Journal of comparative*
381 *neurology*. 2016;524(18):3865-95. doi: 10.1002/cne.24040. PubMed PMID: 27187682; PubMed
382 Central PMCID: PMCPMC5063692.
- 383 2. Zeng H, Sanes JR. Neuronal cell-type classification: challenges, opportunities and the path
384 forward. *Nat Rev Neurosci*. 2017;18(9):530-46. Epub 2017/08/05. doi: 10.1038/nrn.2017.85. PubMed
385 PMID: 28775344.
- 386 3. Bonnavion P, Mickelsen LE, Fujita A, de Lecea L, Jackson AC. Hubs and spokes of the lateral
387 hypothalamus: cell types, circuits and behaviour. *J Physiol*. 2016;594(22):6443-62. doi:
388 10.1113/JP271946. PubMed PMID: 27302606; PubMed Central PMCID: PMCPMC5108896.
- 389 4. Lein ES, Hawrylycz MJ, Ao N, Ayres M, Bensinger A, Bernard A, et al. Genome-wide atlas of
390 gene expression in the adult mouse brain. *Nature*. 2007;445(7124):168-76. doi: 10.1038/nature05453.
391 PubMed PMID: 17151600.
- 392 5. Feng G, Mellor RH, Bernstein M, Keller-Peck C, Nguyen QT, Wallace M, et al. Imaging neuronal
393 subsets in transgenic mice expressing multiple spectral variants of GFP. *Neuron*. 2000;28(1):41-51.
394 Epub 2000/11/22. PubMed PMID: 11086982.
- 395 6. Wickersham IR, Lyon DC, Barnard RJ, Mori T, Finke S, Conzelmann KK, et al. Monosynaptic
396 restriction of transsynaptic tracing from single, genetically targeted neurons. *Neuron*. 2007;53(5):639-
397 47. doi: 10.1016/j.neuron.2007.01.033. PubMed PMID: 17329205; PubMed Central PMCID:
398 PMC2629495.
- 399 7. Boyden ES, Zhang F, Bamberg E, Nagel G, Deisseroth K. Millisecond-timescale, genetically
400 targeted optical control of neural activity. *Nature neuroscience*. 2005;8(9):1263-8. Epub 2005/08/24.
401 doi: 10.1038/nn1525. PubMed PMID: 16116447.
- 402 8. Alexander GM, Rogan SC, Abbas AI, Armbruster BN, Pei Y, Allen JA, et al. Remote control of
403 neuronal activity in transgenic mice expressing evolved G protein-coupled receptors. *Neuron*.
404 2009;63(1):27-39. Epub 2009/07/18. doi: 10.1016/j.neuron.2009.06.014. PubMed PMID: 19607790;
405 PubMed Central PMCID: PMCPmc2751885.
- 406 9. Magnus CJ, Lee PH, Atasoy D, Su HH, Looger LL, Sternson SM. Chemical and genetic engineering
407 of selective ion channel-ligand interactions. *Science (New York, NY)*. 2011;333(6047):1292-6. doi:
408 10.1126/science.1206606. PubMed PMID: 21885782; PubMed Central PMCID: PMCPMC3210548.
- 409 10. Mank M, Santos AF, Drenth S, Mrcic-Flogel TD, Hofer SB, Stein V, et al. A genetically
410 encoded calcium indicator for chronic in vivo two-photon imaging. *Nature methods*. 2008;5(9):805-11.
411 doi: 10.1038/nmeth.1243. PubMed PMID: 19160515.
- 412 11. Mayford M, Bach ME, Huang YY, Wang L, Hawkins RD, Kandel ER. Control of memory formation
413 through regulated expression of a CaMKII transgene. *Science (New York, NY)*. 1996;274(5293):1678-
414 83. PubMed PMID: 8939850.
- 415 12. Shima Y, Sugino K, Hempel CM, Shima M, Taneja P, Bullis JB, et al. A Mammalian enhancer trap
416 resource for discovering and manipulating neuronal cell types. *Elife*. 2016;5:e13503. doi:
417 10.7554/eLife.13503. PubMed PMID: 26999799; PubMed Central PMCID: PMCPMC4846381.
- 418 13. Capecchi MR. Altering the genome by homologous recombination. *Science (New York, NY)*.
419 1989;244(4910):1288-92. Epub 1989/06/16. PubMed PMID: 2660260.
- 420 14. Heintz N. Bac to the future: The use of bac transgenic mice for neuroscience research. *Nat Rev*
421 *Neurosci*. 2001;2(12):861-70.
- 422 15. Huang ZJ. Toward a genetic dissection of cortical circuits in the mouse. *Neuron*.
423 2014;83(6):1284-302. doi: 10.1016/j.neuron.2014.08.041. PubMed PMID: 25233312; PubMed Central
424 PMCID: PMC4169123.
- 425 16. Madisen L, Garner AR, Shimaoka D, Chuong AS, Klapoetke NC, Li L, et al. Transgenic mice for
426 intersectional targeting of neural sensors and effectors with high specificity and performance. *Neuron*.
427 2015;85(5):942-58. doi: 10.1016/j.neuron.2015.02.022. PubMed PMID: 25741722; PubMed Central
428 PMCID: PMCPMC4365051.

- 429 17. Luo L, Callaway EM, Svoboda K. Genetic dissection of neural circuits. *Neuron*. 2008;57(5):634-
430 60. doi: 10.1016/j.neuron.2008.01.002. PubMed PMID: 18341986; PubMed Central PMCID:
431 PMCPMC2628815.
- 432 18. Banerji J, Rusconi S, Schaffner W. Expression of a beta-globin gene is enhanced by remote SV40
433 DNA sequences. *Cell*. 1981;27(2 Pt 1):299-308. Epub 1981/12/01. PubMed PMID: 6277502.
- 434 19. ENCODE PC. An integrated encyclopedia of DNA elements in the human genome. *Nature*.
435 2012;489(7414):57-74. doi: 10.1038/nature11247. PubMed PMID: 22955616; PubMed Central PMCID:
436 PMC3439153.
- 437 20. Roadmap Epigenomics C, Kundaje A, Meuleman W, Ernst J, Bilenky M, Yen A, et al. Integrative
438 analysis of 111 reference human epigenomes. *Nature*. 2015;518(7539):317-30. Epub 2015/02/20. doi:
439 10.1038/nature14248. PubMed PMID: 25693563; PubMed Central PMCID: PMCPMC4530010.
- 440 21. Yasuda M, Mayford MR. CaMKII activation in the entorhinal cortex disrupts previously encoded
441 spatial memory. *Neuron*. 2006;50(2):309-18. doi: 10.1016/j.neuron.2006.03.035. PubMed PMID:
442 16630840.
- 443 22. Heintzman ND, Stuart RK, Hon G, Fu Y, Ching CW, Hawkins RD, et al. Distinct and predictive
444 chromatin signatures of transcriptional promoters and enhancers in the human genome. *Nature*
445 *genetics*. 2007;39(3):311-8. doi: 10.1038/ng1966. PubMed PMID: 17277777.
- 446 23. Visel A, Rubin EM, Pennacchio LA. Genomic views of distant-acting enhancers. *Nature*.
447 2009;461(7261):199-205. doi: 10.1038/nature08451. PubMed PMID: 19741700; PubMed Central
448 PMCID: PMC2923221.
- 449 24. Visel A, Taher L, Girgis H, May D, Golonzhka O, Hoch RV, et al. A high-resolution enhancer atlas
450 of the developing telencephalon. *Cell*. 2013;152(4):895-908. doi: 10.1016/j.cell.2012.12.041. PubMed
451 PMID: 23375746; PubMed Central PMCID: PMC3660042.
- 452 25. Cotney J, Leng J, Yin J, Reilly SK, DeMare LE, Emera D, et al. The evolution of lineage-specific
453 regulatory activities in the human embryonic limb. *Cell*. 2013;154(1):185-96. Epub 2013/07/06. doi:
454 10.1016/j.cell.2013.05.056
- 455 S0092-8674(13)00699-5 [pii]. PubMed PMID: 23827682; PubMed Central PMCID: PMC3785101.
- 456 26. Visel A, Blow MJ, Li Z, Zhang T, Akiyama JA, Holt A, et al. ChIP-seq accurately predicts tissue-
457 specific activity of enhancers. *Nature*. 2009;457(7231):854-8. doi: 10.1038/nature07730. PubMed
458 PMID: 19212405; PubMed Central PMCID: PMCPMC2745234.
- 459 27. Shen Y, Yue F, McCleary DF, Ye Z, Edsall L, Kuan S, et al. A map of the cis-regulatory sequences
460 in the mouse genome. *Nature*. 2012;488(7409):116-20. doi: 10.1038/nature11243. PubMed PMID:
461 22763441; PubMed Central PMCID: PMCPMC4041622.
- 462 28. McLean CY, Bristor D, Hiller M, Clarke SL, Schaar BT, Lowe CB, et al. GREAT improves functional
463 interpretation of cis-regulatory regions. *Nature biotechnology*. 2010;28(5):495-501. doi:
464 10.1038/nbt.1630. PubMed PMID: 20436461; PubMed Central PMCID: PMCPMC4840234.
- 465 29. Gossen M, Bujard H. Tight control of gene expression in mammalian cells by tetracycline-
466 responsive promoters. *Proceedings of the National Academy of Sciences of the United States of*
467 *America*. 1992;89(12):5547-51. Epub 1992/06/15. PubMed PMID: 1319065; PubMed Central PMCID:
468 PMCPMC49329.
- 469 30. Brand AH, Perrimon N. Targeted gene expression as a means of altering cell fates and
470 generating dominant phenotypes. *Development*. 1993;118(2):401-15. PubMed PMID: 8223268.
- 471 31. Weible AP, Moore AK, Liu C, DeBlander L, Wu H, Kentros C, et al. Perceptual gap detection is
472 mediated by gap termination responses in auditory cortex. *Current biology : CB*. 2014;24(13):1447-55.
473 doi: 10.1016/j.cub.2014.05.031. PubMed PMID: 24980499; PubMed Central PMCID:
474 PMCPMC4131718.
- 475 32. Witter MP, Doan TP, Jacobsen B, Nilssen ES, Ohara S. Architecture of the Entorhinal Cortex A
476 Review of Entorhinal Anatomy in Rodents with Some Comparative Notes. *Front Syst Neurosci*.
477 2017;11:46. doi: 10.3389/fnsys.2017.00046. PubMed PMID: 28701931; PubMed Central PMCID:
478 PMCPMC5488372.

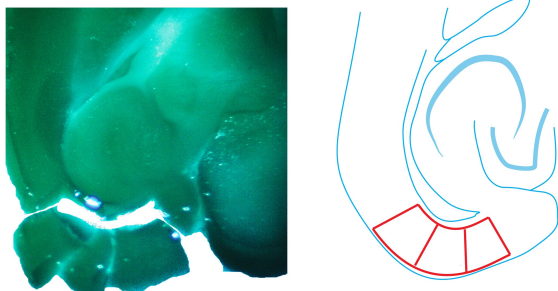
- 479 33. DeFelipe J, Lopez-Cruz PL, Benavides-Piccione R, Bielza C, Larranaga P, Anderson S, et al. New
480 insights into the classification and nomenclature of cortical GABAergic interneurons. *Nat Rev Neurosci*.
481 2013;14(3):202-16. doi: 10.1038/nrn3444. PubMed PMID: 23385869; PubMed Central PMCID:
482 PMCPMC3619199.
- 483 34. Taniguchi H. Genetic dissection of GABAergic neural circuits in mouse neocortex. *Frontiers in*
484 *cellular neuroscience*. 2014;8:8. doi: 10.3389/fncel.2014.00008. PubMed PMID: 24478631; PubMed
485 Central PMCID: PMC3902216.
- 486 35. Tasic B, Menon V, Nguyen TN, Kim TK, Jarsky T, Yao Z, et al. Adult mouse cortical cell taxonomy
487 revealed by single cell transcriptomics. *Nature neuroscience*. 2016;19(2):335-46. doi:
488 10.1038/nn.4216. PubMed PMID: 26727548; PubMed Central PMCID: PMCPMC4985242.
- 489 36. Briggs F, Callaway EM. Layer-specific input to distinct cell types in layer 6 of monkey primary
490 visual cortex. *The Journal of neuroscience : the official journal of the Society for Neuroscience*.
491 2001;21(10):3600-8. PubMed PMID: 11331389; PubMed Central PMCID: PMCPMC1820845.
- 492 37. Reilly SK, Yin J, Ayoub AE, Emera D, Leng J, Cotney J, et al. Evolutionary genomics. Evolutionary
493 changes in promoter and enhancer activity during human corticogenesis. *Science (New York, NY)*.
494 2015;347(6226):1155-9. doi: 10.1126/science.1260943. PubMed PMID: 25745175; PubMed Central
495 PMCID: PMCPMC4426903.
- 496 38. Vermunt MW, Reinink P, Korving J, de Bruijn E, Creyghton PM, Basak O, et al. Large-scale
497 identification of coregulated enhancer networks in the adult human brain. *Cell Rep*. 2014;9(2):767-79.
498 doi: 10.1016/j.celrep.2014.09.023. PubMed PMID: 25373911.
- 499 39. Gray LT, Yao Z, Nguyen TN, Kim TK, Zeng H, Tasic B. Layer-specific chromatin accessibility
500 landscapes reveal regulatory networks in adult mouse visual cortex. *Elife*. 2017;6. doi:
501 10.7554/eLife.21883. PubMed PMID: 28112643; PubMed Central PMCID: PMCPMC5325622.
- 502 40. Luo C, Keown CL, Kurihara L, Zhou J, He Y, Li J, et al. Single-cell methylomes identify neuronal
503 subtypes and regulatory elements in mammalian cortex. *Science (New York, NY)*. 2017;357(6351):600-
504 4. Epub 2017/08/12. doi: 10.1126/science.aan3351. PubMed PMID: 28798132; PubMed Central
505 PMCID: PMCPMC5570439.
- 506 41. Dimidschstein J, Chen Q, Tremblay R, Rogers SL, Saldi GA, Guo L, et al. A viral strategy for
507 targeting and manipulating interneurons across vertebrate species. *Nature neuroscience*.
508 2016;19(12):1743-9. doi: 10.1038/nn.4430. PubMed PMID: 27798629; PubMed Central PMCID:
509 PMCPMC5348112.
- 510 42. Prabhakar S, Visel A, Akiyama JA, Shoukry M, Lewis KD, Holt A, et al. Human-specific gain of
511 function in a developmental enhancer. *Science (New York, NY)*. 2008;321(5894):1346-50. Epub
512 2008/09/06. doi: 10.1126/science.1159974. PubMed PMID: 18772437; PubMed Central PMCID:
513 PMCPMC2658639.
- 514 43. Nord AS, Blow MJ, Attanasio C, Akiyama JA, Holt A, Hosseini R, et al. Rapid and pervasive
515 changes in genome-wide enhancer usage during mammalian development. *Cell*. 2013;155(7):1521-31.
516 Epub 2013/12/24. doi: 10.1016/j.cell.2013.11.033. PubMed PMID: 24360275; PubMed Central PMCID:
517 PMCPMC3989111.
- 518 44. Pattabiraman K, Golonzhka O, Lindtner S, Nord AS, Taher L, Hoch R, et al. Transcriptional
519 regulation of enhancers active in protodomains of the developing cerebral cortex. *Neuron*.
520 2014;82(5):989-1003. doi: 10.1016/j.neuron.2014.04.014. PubMed PMID: 24814534; PubMed Central
521 PMCID: PMC4104757.
- 522 45. Silberberg SN, Taher L, Lindtner S, Sandberg M, Nord AS, Vogt D, et al. Subpallial Enhancer
523 Transgenic Lines: a Data and Tool Resource to Study Transcriptional Regulation of GABAergic Cell Fate.
524 *Neuron*. 2016;92(1):59-74. doi: 10.1016/j.neuron.2016.09.027. PubMed PMID: 27710791; PubMed
525 Central PMCID: PMCPMC5063253.
- 526 46. Merkle FT, Alvarez-Buylla A. Neural stem cells in mammalian development. *Curr Opin Cell Biol*.
527 2006;18(6):704-9. doi: 10.1016/j.ceb.2006.09.008. PubMed PMID: 17046226.
- 528 47. Fogarty M, Grist M, Gelman D, Marin O, Pachnis V, Kessar N. Spatial genetic patterning of the
529 embryonic neuroepithelium generates GABAergic interneuron diversity in the adult cortex. *The Journal*

- 530 of neuroscience : the official journal of the Society for Neuroscience. 2007;27(41):10935-46. doi:
531 10.1523/JNEUROSCI.1629-07.2007. PubMed PMID: 17928435.
- 532 48. Zerucha T, Stuhmer T, Hatch G, Park BK, Long Q, Yu G, et al. A highly conserved enhancer in
533 the Dlx5/Dlx6 intergenic region is the site of cross-regulatory interactions between Dlx genes in the
534 embryonic forebrain. *The Journal of neuroscience : the official journal of the Society for Neuroscience.*
535 2000;20(2):709-21. Epub 2000/01/13. PubMed PMID: 10632600.
- 536 49. Kanter BR, Lykken CM, Avesar D, Weible A, Dickinson J, Dunn B, et al. A Novel Mechanism for
537 the Grid-to-Place Cell Transformation Revealed by Transgenic Depolarization of Medial Entorhinal
538 Cortex Layer II. *Neuron.* 2017;93(6):1480-92 e6. Epub 2017/03/24. doi: 10.1016/j.neuron.2017.03.001.
539 PubMed PMID: 28334610.
- 540 50. Harris KD, Shepherd GM. The neocortical circuit: themes and variations. *Nature neuroscience.*
541 2015;18(2):170-81. doi: 10.1038/nn.3917. PubMed PMID: 25622573; PubMed Central PMCID:
542 PMC4889215.
- 543 51. Douglas RJ, Martin KA. Recurrent neuronal circuits in the neocortex. *Current biology : CB.*
544 2007;17(13):R496-500. doi: 10.1016/j.cub.2007.04.024. PubMed PMID: 17610826.
- 545 52. Tasic B, Yao Z, Smith KA, Graybiel LT, T.N. N, Bertagnoli D, et al. Shared and distinct
546 transcriptomic cell types across neocortical areas. *bioRxiv.* 2017. doi:
547 <http://dx.doi.org/10.1101/229542>.
- 548 53. Fuchs EC, Neitz A, Pinna R, Melzer S, Caputi A, Monyer H. Local and Distant Input Controlling
549 Excitation in Layer II of the Medial Entorhinal Cortex. *Neuron.* 2016;89(1):194-208. doi:
550 10.1016/j.neuron.2015.11.029. PubMed PMID: 26711115; PubMed Central PMCID: PMC4712190.
- 551 54. Malik AN, Vierbuchen T, Hemberg M, Rubin AA, Ling E, Couch CH, et al. Genome-wide
552 identification and characterization of functional neuronal activity-dependent enhancers. *Nature*
553 *neuroscience.* 2014;17(10):1330-9. doi: 10.1038/nn.3808. PubMed PMID: PMC4297619.

554

Figure 1.

A Microdissect brain regions



B Apply ChIP-seq to identify regionally specific enhancers



C Clone single enhancers into transgenic construct



D Create transgenic animals with regionally specific transgene expression

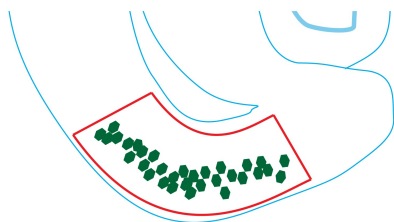


Figure 1. Experimental summary of Enhancer Driven Gene Expression (EDGE). (A) Samples of brain regions of interest are microdissected by hand. (B) ChIP-seq is performed on these samples and genome-wide H3K27ac and H3K4me2 signals for each sample are compared to reference signals and signals from the other samples. Bioinformatic analysis algorithms output unique peaks as potential region-specific enhancers (red bar). (C) Single putative enhancers are cloned into constructs containing a heterologous minimal promoter to drive transgene expression. (D) Following pronuclear injection of these constructs, the resulting founder mice are crossed to reporter lines and evaluated for desired expression patterns.

Figure 2

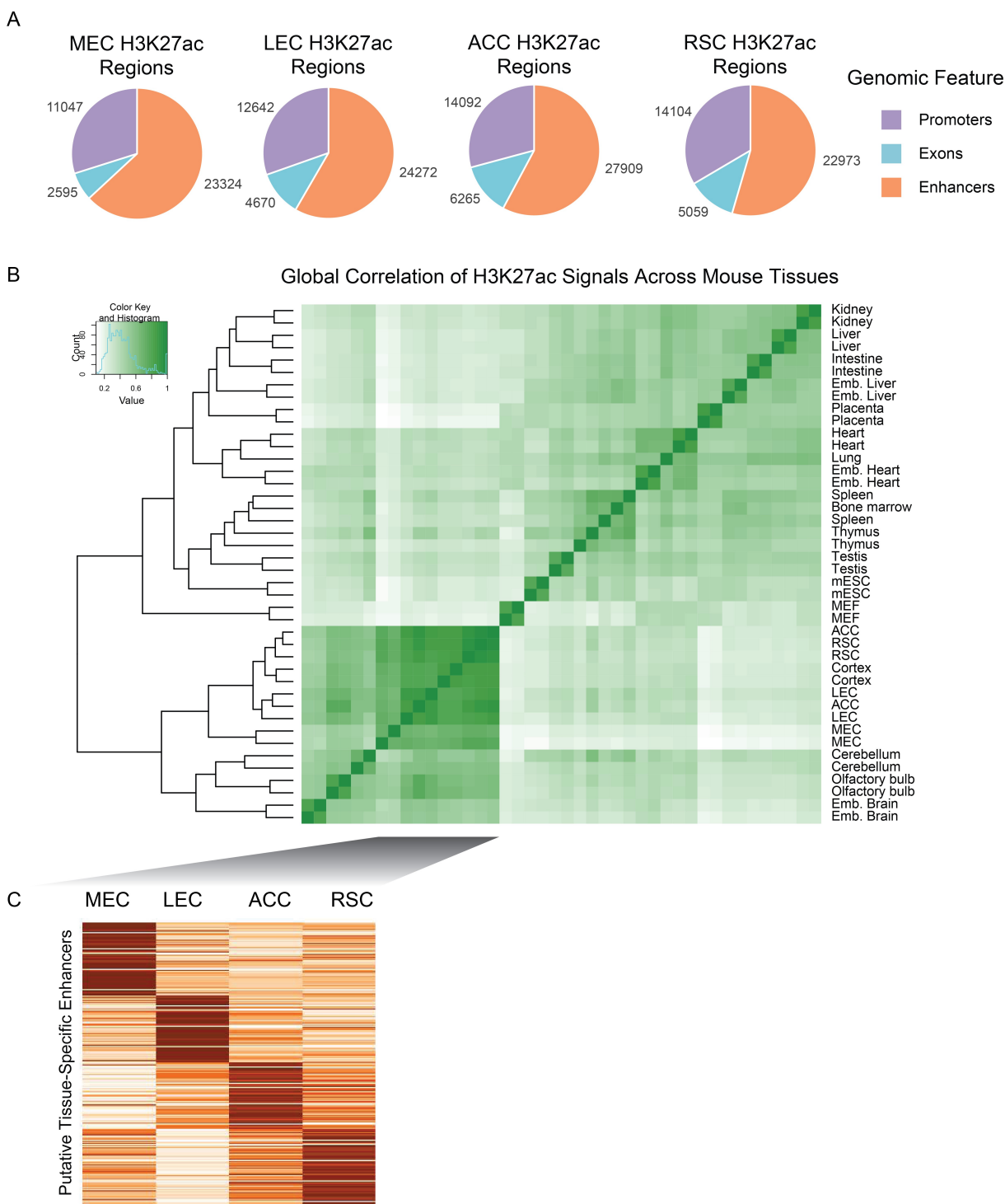


Figure 2. ChIP-seq reveals a striking diversity of unique and novel enhancers in different cortical sub-regions. (A) Pie charts showing the proportions (and numbers) of distinct active genomic elements identified by H2K27ac ChIP-seq of the 4 cortical subregions. These numbers are roughly similar to those found by ChIP-seq of other organs. (B) Dendrogram (left) and correlation matrix of the H3K27ac signals (right) from replicates of the cortical subregions dissected in this experiment versus those from ENCODE were used for subtraction. Note the high correlation of replicates and clustering of signal from cortical tissues. (C) Heatmaps showing some of the tissue-specific putative enhancers identified in the microdissected cortical subregions.

Figure 3.

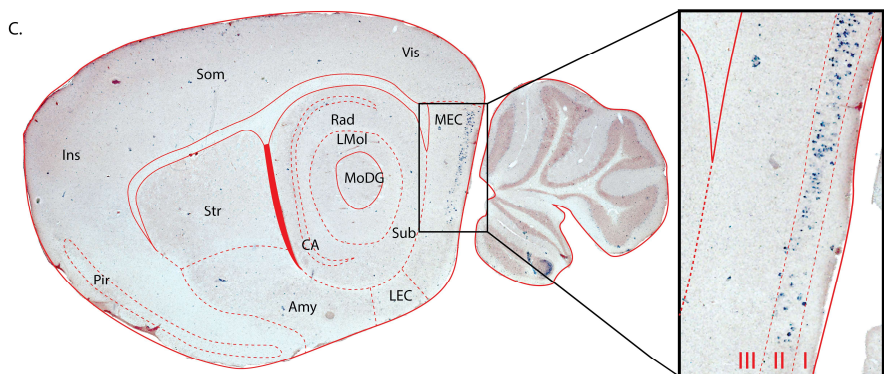
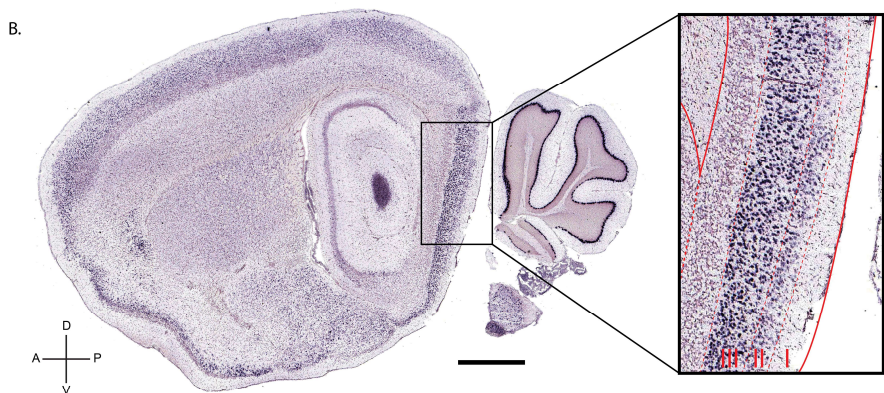
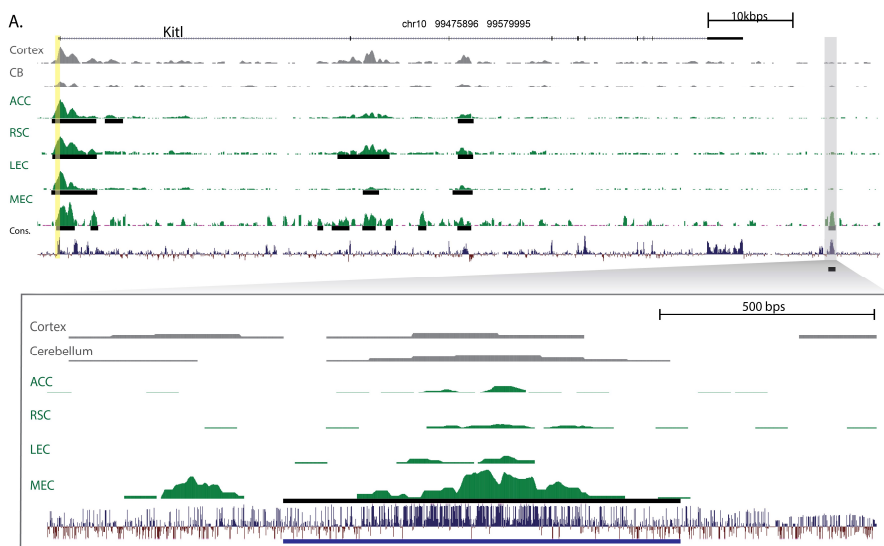
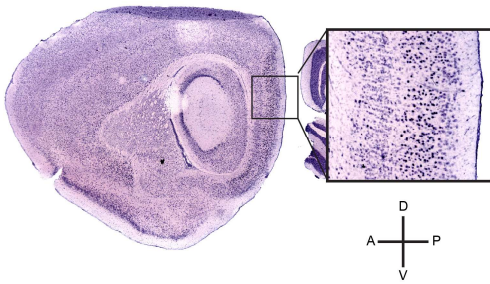


Figure 3. The enhancers of non-specific genes drive region-specific transgene expression. (A) A genomic view of one of the 165 MEC-specific enhancers yielded by ChIP-seq analysis. The top panel indicates the location and coding regions of *Kitl* as well as H3K27Ac signal for two regions from Roadmap epigenome (Cortex and Cerebellum), the four regions we analyzed (ACC, RSC, LEC and MEC), and conservation over 30 species. The vertical yellow column indicates the promoter region upstream of the transcriptional start site. Peak calls are denoted by the black horizontal lines. The specific genomic region containing the enhancer (MEC-13-81) is blown up in the bottom panel. (B) ISH (brain-map.org) of *Kitl*, the gene associated with enhancer MEC-13-81 shows expression throughout cortex, hippocampus and cerebellum. (C) tTA dependent transgene Arch driven by the enhancer (ranked number 81) is expressed in MEC LII. Scalebar is 1000 μ m. Sagittal plane, Dorsal-Ventral and Anterior-Posterior axis are indicated. Abbreviations are: Ins: insular cortex, Som: somatosensory cortex, Vis: visual cortex, Pir: Piriform cortex, Str: striatum, Amy: amygdala and associated regions, Rad: stratum radiatum of the hippocampus, LMol: molecular layer of the hippocampus, CA: both cornu ammonis fields of the hippocampus, sub: subiculum, MoDG: molecular layer of the Dentate Gyrus, LEC: lateral

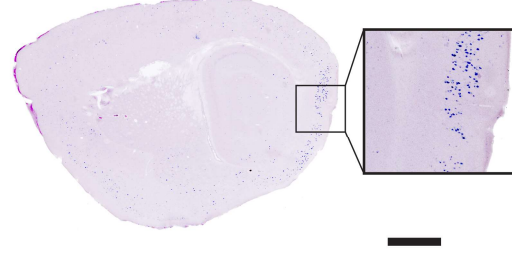
entorhinal cortex, MEC: medial entorhinal cortex, Layers I, II and III of the MEC are indicated in the blow-up to the right.

Figure 4.

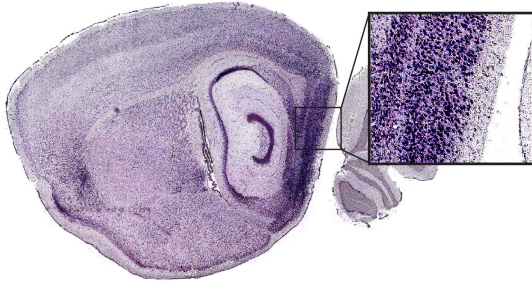
A *Atp10a*



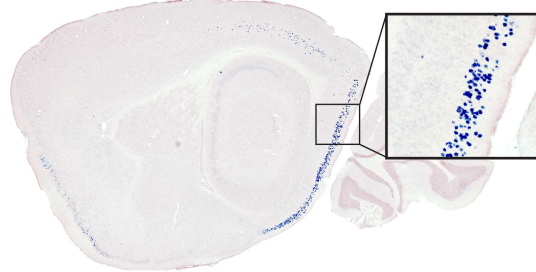
Enhancer MEC-13-32B (TVAG)



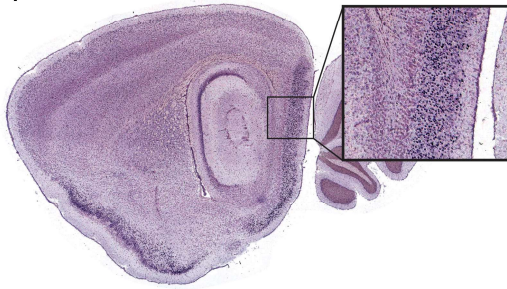
B *Odz3*



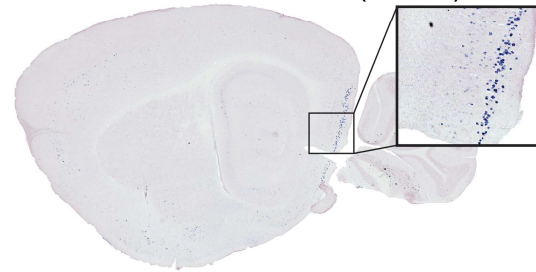
Enhancer MEC-13-53A (HM3)



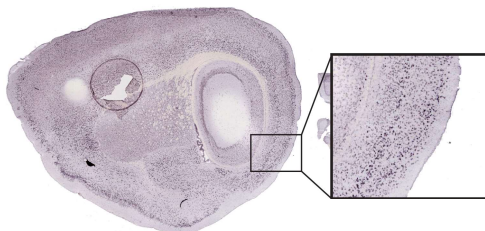
C *Trps1*



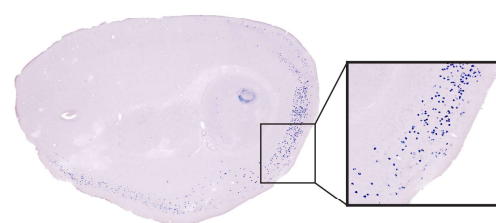
Enhancer MEC-13-104B (TVAG)



D *Dok5*



Enhancer LEC-13-8A (GC6)



E *Nos1*



Enhancer LEC-13-108A (GC6)

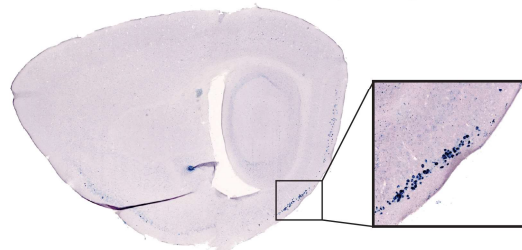


Figure 4. Distinct MEC-specific enhancers drive transgene expression in distinct sets of cells in MEC. (A through E, left column) ISH showing expression patterns of native genes associated with EC-specific enhancers. (A through E, right column) ISH showing EC-specific expression of transgenes driven by the corresponding EC-specific enhancers, tTA driven transgenes in parentheses. ISH for the native genes from brain-map.org. Scalebar in A is 1000 μ m.

Figure 5.

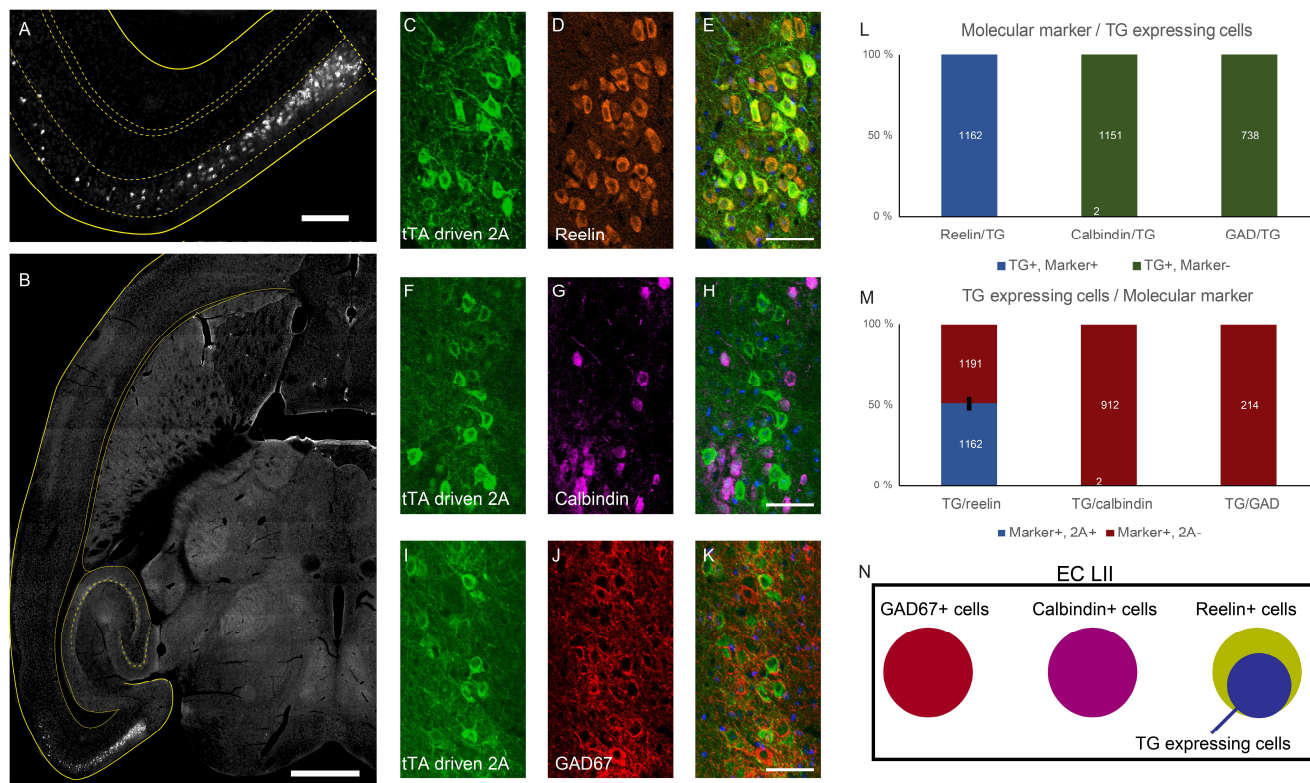


Figure 5. Single enhancers can drive expression in histochemically-defined subsets of MEC LII cells. (A,B) Horizontal section of a mouse cross between MEC-13-53A and TVAG. Immunohistochemical transgene detection with anti-2A Ab shows layer II EC-specific expression. (C,F,I) Anti-2A histochemistry; (D) Anti-Reelin; (G) Anti-Calbindin; (J) Anti-GAD67; (E,H,K) Overlays of the two signals, each row is the same section. (L) 100% (1162/1162 counted cells) of transgenic cells co-localize with Reelin but there is essentially 0% co-localization with calbindin (2/1151) and GAD67 (0/738). (M) 49.4% (1162/2353) of all Reelin positive cells were positive for the transgene, essentially none of the other cell populations had any transgene expressing cells. Total numbers of cells counted in white. (N) Schematic summary of the data in C to M. Scale bars are 1000 μ m in B, 200 μ m in A and 50 μ m in C-K. In all graphs bars show the mean \pm SEM.

Figure 6.

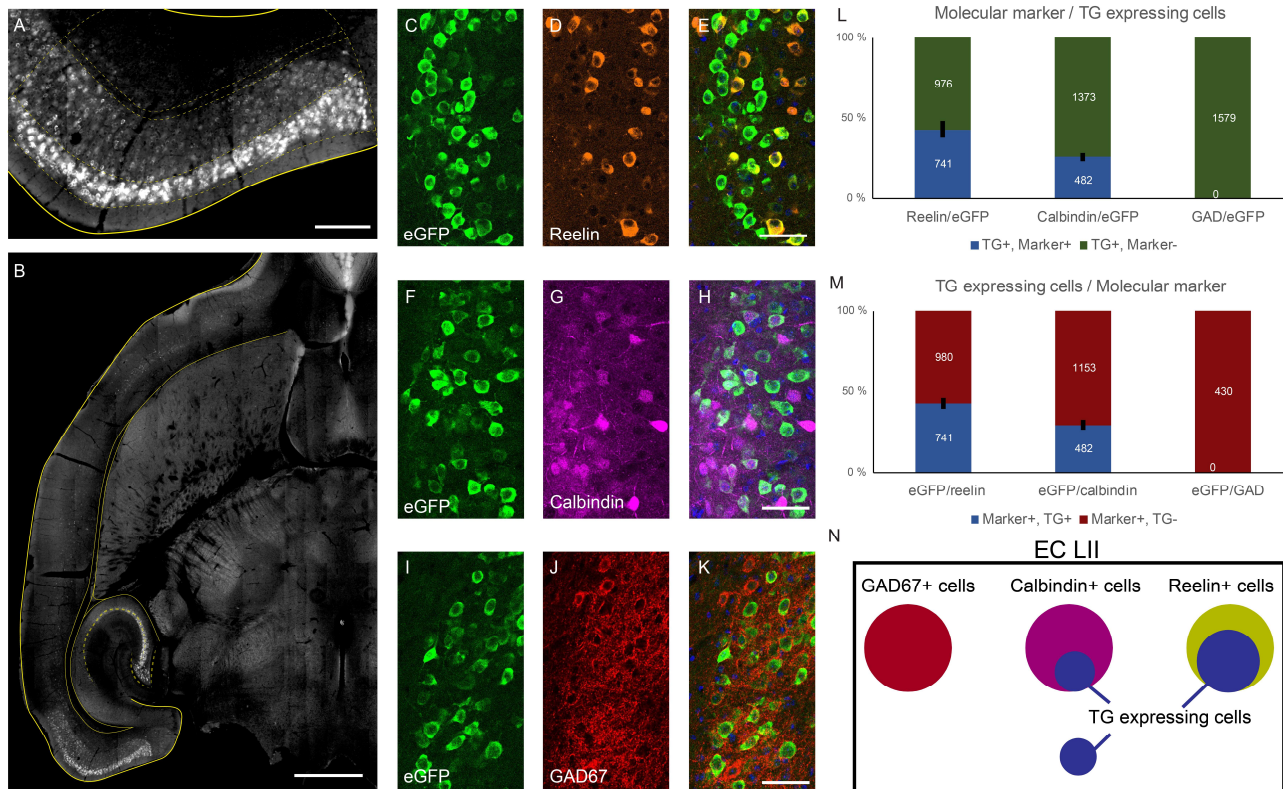
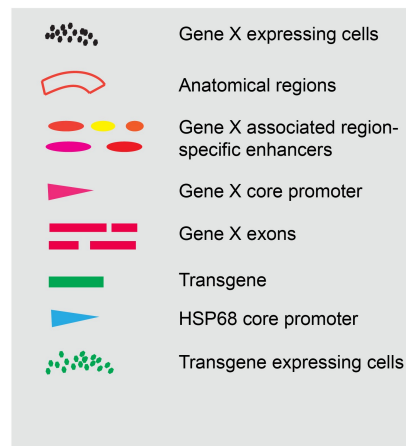
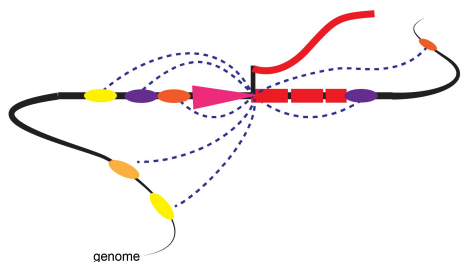
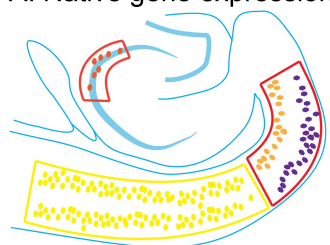


Figure 6. Different single enhancers can drive expression in histochemically-distinct subsets of MEC LII cells. (A,B) Horizontal section of a mouse cross between MEC-13-104B and tetO-eGFP. Immunohistochemical transgene detection with anti-GFP Ab shows expression in layer II of the EC. (C,F,I) Anti-GFP histochemistry; (D) Anti-Reelin; (G) Anti-Calbindin; (J) Anti-GAD67; (E,H,K) Overlays of the two signals, each row is the same section. (L) 43.1% (741/1717 counted cells) of transgenic cells in layer II of the EC co-localize with Reelin while 26% (482/1855) of them co-localize with calbindin. 0% (0/1579) co-localize with GAD67. (M) 43.1% (741/1721) of all Reelin positive cells in layer II of the EC were positive for the transgene and 28.5% (482/1635) of all Calbindin positive cells in layer II of the EC were positive for the transgene, while 0% (0/430) of the GAD67 positive population had any transgene expressing cells. Total numbers of cells counted in white. (N) Schematic summary of the data in C to M. Scale bars are 1000 μ m in B, 200 μ m in A and 50 μ m in C-K. In all graphs bars show the mean \pm SEM.

Figure 7.

A. Native gene expression



B. Enhancer Driven Gene Expression

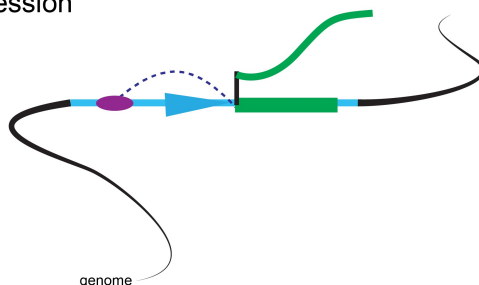
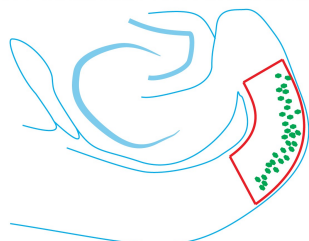
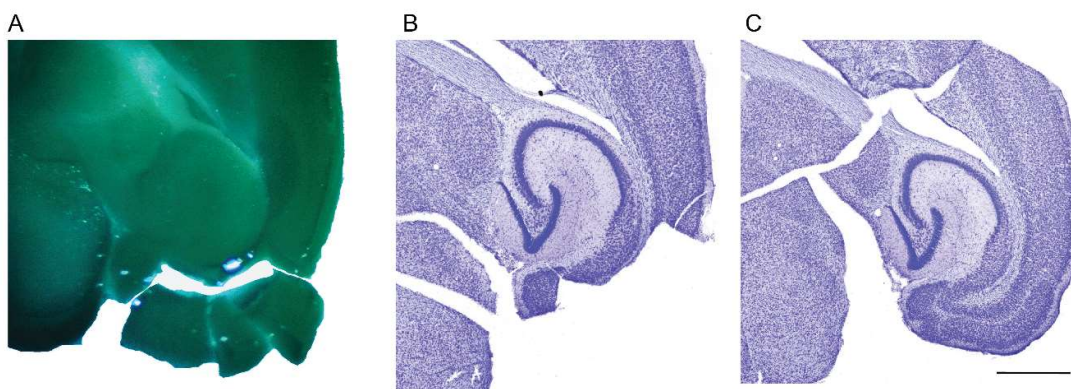


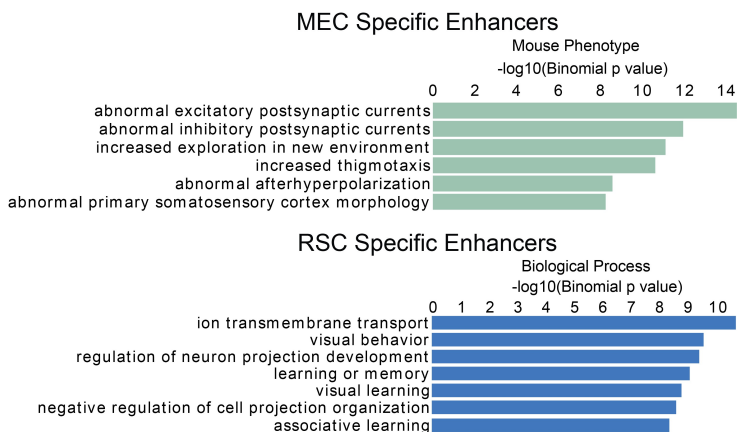
Figure 7. Schematic of putative genetic basis for EDGE technology. (A) Native gene expression: A gene “X” is expressed in multiple cell types in distinct brain areas. Expression in each cell type is driven by distinct sets of color-coded active enhancers acting upon the native core promoter (pink triangle). Promoter-based methods of transgene expression such as BAC transgenesis and Knock-ins respectively include several or all of the native enhancers, thereby recapitulating some or all of the expression pattern of the native gene. (B) Enhancer-Driven Gene Expression: a single active enhancer isolated from a particular brain region drives transgene expression from a heterologous minimal promoter (blue). This leads to transgene expression that is restricted to a particular region-specific subset of the cell types that the native promoter expresses in, greatly increasing the anatomical specificity relative to promoter-based methods or the native gene.

Supplemental figure 1



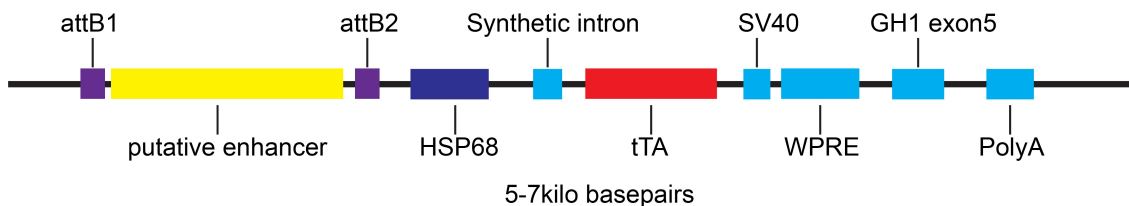
Supplemental figure 1. Example of microdissection (A) 500µm thick section during microdissection. (B) Contralateral side of the same section as in (A), re-sectioned to 50µm and Nissl stained. (C) Re-sectioned (50µm), Nissl stained tissue from (A). Scalebar is 1000µm

Supplemental figure 2



Supplemental figure 2. Gene Ontology of selected cortical subregions.

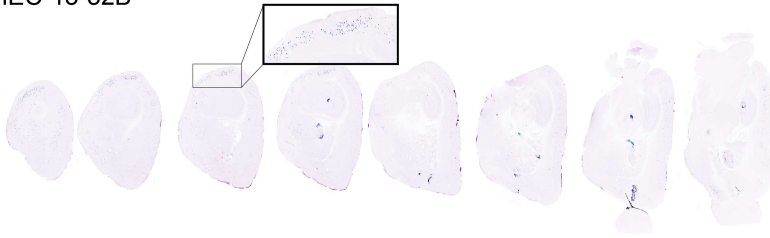
Supplemental figure 3



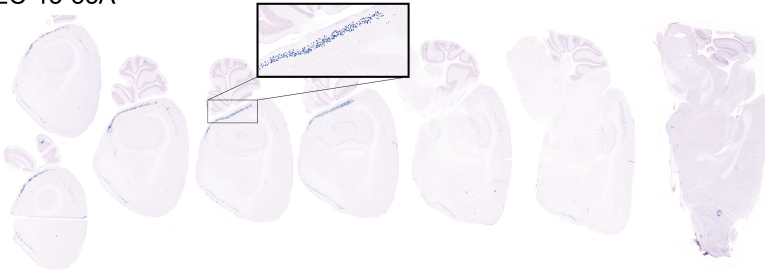
Supplemental figure 3. Injection construct. The putative enhancer of 0.7 to 3kbp was cloned to the injection construct by gateway® cloning. The synthetic intron, SV40, WPRE and growth hormone 1 exon 5 are present for optimal mRNA stability and expression of the tetracycline TransActivator (tTA). The construct is linearized with appropriate restriction enzymes depending on exact sequence of the putative enhancer.

Supplemental figure 4.

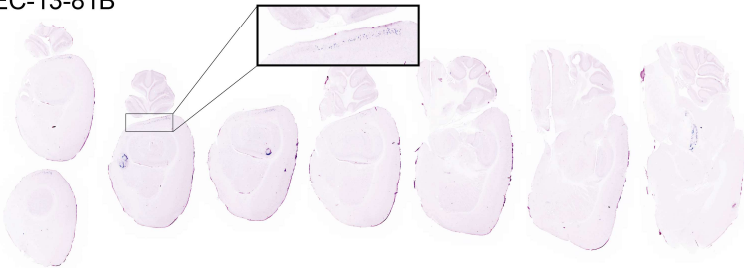
MEC-13-32B



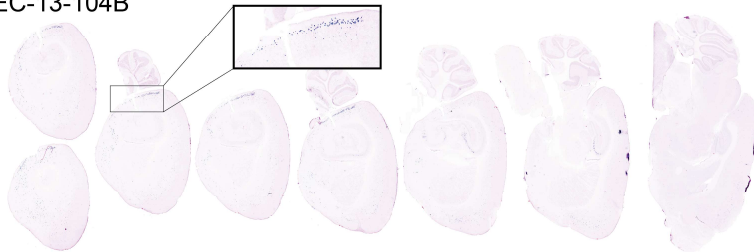
MEC-13-53A



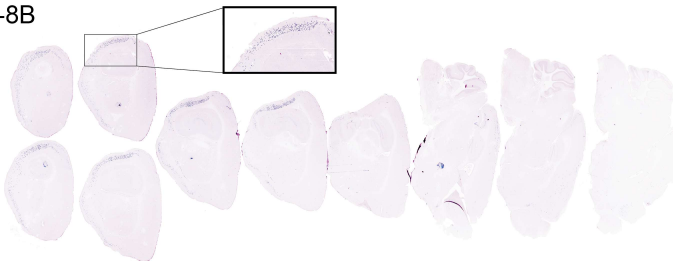
MEC-13-81B



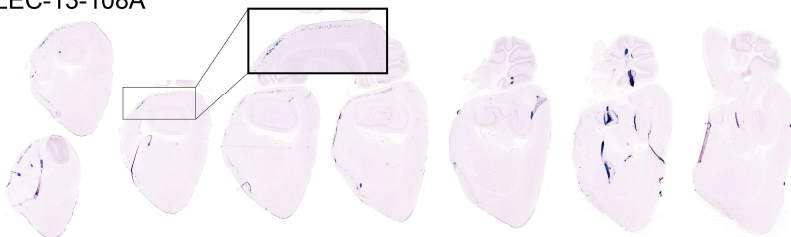
MEC-13-104B



LEC-13-8B



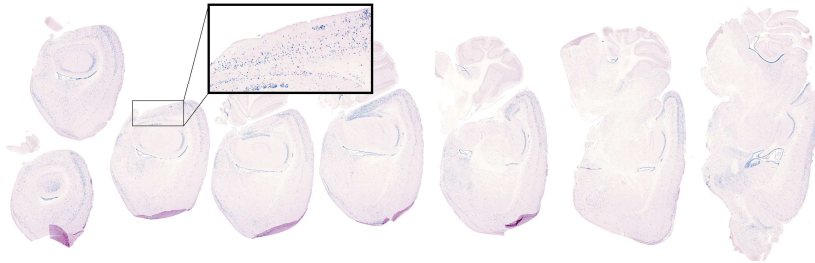
LEC-13-108A



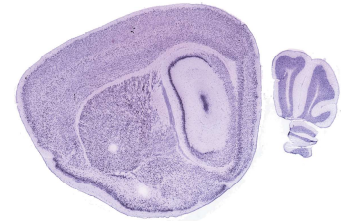
Supplemental figure 4. Extended medial lateral coverage of sagittal sections shown in figures 3 and 4. Enhancer lines based 6 different enhancers used (MEC-13-32B, MEC-13-53A, MEC-13-81B, MEC-13-104B, LEC-13-8B, LEC-13-108A) show specific transgene expression in the EC.

Supplemental figure 5.

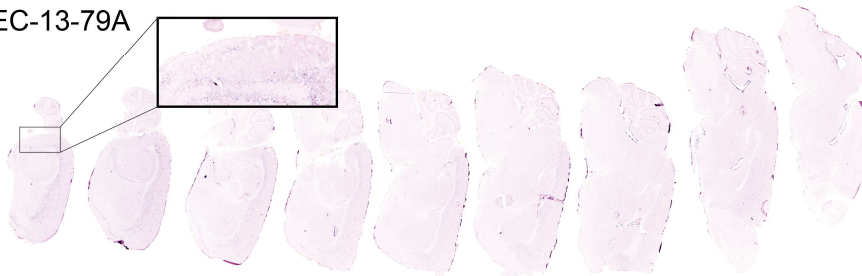
MEC-13-48E



Phactr1



MEC-13-79A



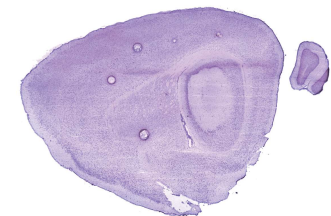
Fam5C



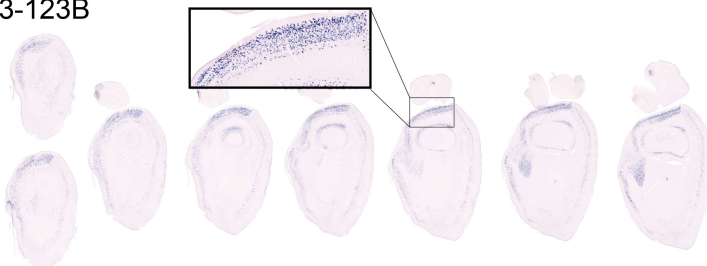
MEC-13-95F



Mgst1



MEC-13-123B



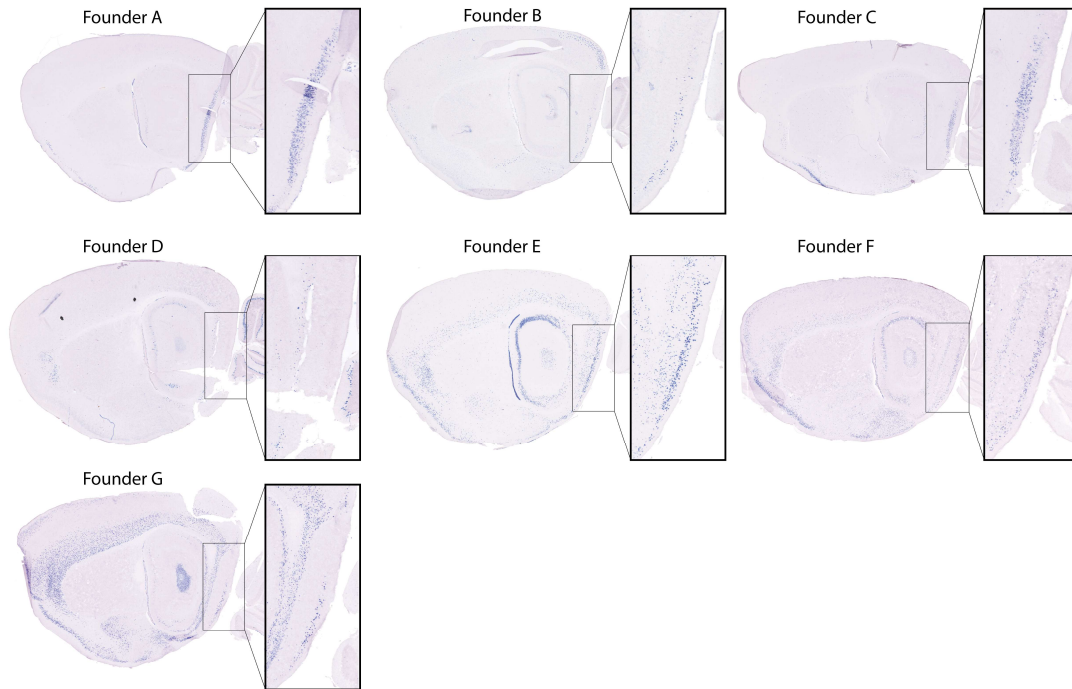
Igsf11



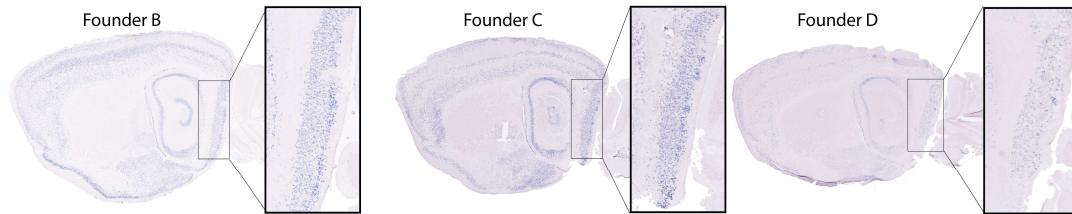
Supplemental figure 5. Expression of enhancer driven transgenes by 4 unique EC enhancers not shown in the main figures. Enhancer lines based on 4 different enhancers (MEC-13-48E, MEC-13-79A, MEC-13-95F, MEC-13-123B) show enriched, but not specific transgene expression in the EC. The right column shows *in situ hybridization* (taken from brain-map.org) of associated genes.

Supplemental figure 6.

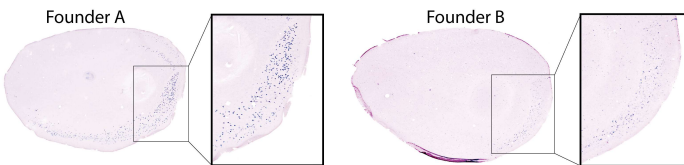
A. Enhancer MEC-13-53



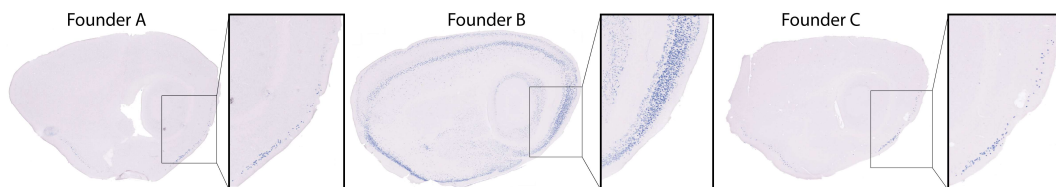
B. Enhancer MEC-13-123



C. Enhancer LEC-13-8



D. Enhancer LEC-13-108



Supplemental figure 6. Enhancer driven transgene expression of various genomic insertions. Sagittal sections of approximately similar levels. Different founders based on the same enhancers show roughly similar expression patterns. All mice based on MEC specific enhancers were crosses with hGFP reporter mice, while all mice based on LEC specific enhancers were crossed with GC6 payload mice. (A) Enhancer MEC-13-53 reproducibly shows expression in LI of the EC in 6 of the 7 analyzed mouse lines. We do find expression in other regions, such as visual cortex in founder

B, the CA fields of the hippocampus in founder E, and deep layers of cortex in founder G. But since all of these patterns of expression occur only once within the 7 analyzed lines, we consider them to be positional effects. (B) Enhancer MEC-13-123 reproducibly shows expression in LIII of the EC, CA3 and select cortical layers. (C) Enhancer LEC-13-8 reproducibly shows expression in LIII of the EC. (D) Enhancer LEC-13-108 reproducibly shows expression in LII of the EC. We consider the additional expression in the “founder B” line to be another positional effect.

Supplemental table 1. Ranked regionally specific enhancers for brain regions MEC, LEC, ACC and RSC.

-----Attached file-----

Supplemental table 2. Overview of generated transgenic lines. Genomic coordinates are in mm9 and indicate the exact region used for the enhancer in the transgenic construct, rather than the putative enhancer as indicated by ChIP-seq. Enhancer rank indicates the rank as a result of the ChIP-seq analysis. Associated genes are a result of analysis of GREAT. All indications of expression are based on the initial round of assessment where mice based on MEC specific enhancers were crossed with histone GFP reporter mice and mice based on LEC specific enhancers were crossed with gCaMP6. The numbers in the last column are taken from Shima et al. 2016, table 1 and supplemental table 1 to identify the lines expressing in the EC (53L, 56L, TCAO, TCAR, TCIF, TCLC).

Genomic coordinates enhancer	chr1:148,339,12 9-148,340,300	chr16:39,750,78 9-39,753,454	chr10:99,573,05 1-99,574,981	chr15:50,913,89 6-50,916,356	chr7:65,916,19 8-65,918,580	chr6:138,334,72 8-138,335,952	chr8:49,906,38 8-49,908,569	chr13:42,782,50 3-42,784,035	MEC	chr2:171,158,07 9-171,159,156	chr5:118,194,6 53-118,195,333	LEC	Shima et al.
Enhancer rank	79	123	81	104	32	95	53	48		8	108		
Associated genes	Fam5c	Igsf11	Kitl Gm4301	Trps1 Eif3h	Ube3a Atp10a	Lmo3 Mgst1	Odz3	Phactr1 Tbc1d7	total	Dok5 Cbln4	Nos1 Ksr2	total	variable integration
tTA positive founders	6	6	10	12	8	16	18	20	96	5	4	9	151
Lines analyzed	5	4	7	8	4	13	16	16	73	4	3	7	151
GFP signal in EC	2	4	3	3	3	7	7	7	36	2	3	5	6
No GFP signal in brain	2	0	4	4	1	5	9	8	33	2	0	2	109
GFP in brain but no GFP in EC	1	0	0	1	0	1	0	1	4	0	0	0	36

Supplemental table 3. Primers used for genotyping. All primers were used in a concentration of 10µM. All genes are genotyped individually, ie. tTA x TVAG crosses were genotyped using two separate reactions, one for tTA and one for TVAG.

Gene	Primer 1 (5'-3')	Primer 2 (5'-3')	Product size (bp)	Internal control primer 1 (5'-3')	Internal control primer 2 (5'-3')	Product size (bp)
tTA	GGACAAGTCCAAGGTGA TCAAC	CCTGGTGGTCGAACAG CTCG	591	CTA GGC CAC AGA ATT GAA AGA TCT	GTA GGT GGA AAT TCT AGC ATC ATC C	324
Histone GFP	TGGGGACGGTGATGC GGTCT	ACGTGGCGAAGCTCTG CTGC	~300	CAA ATG TTG CTT GTC TGG TG	GTC AGT CGA GTG CAC AGT TT	200
TVAG	GTCCGGTAACGGTTC TTTG	GCTCTGTGTCAGGCACC AG	391	CGT CTT TAA TTG GAT TAC AAT GCT	CTA GCA AGT GGT TGT GGT CA	181
Arch	CTTCTCGCTAAGGTG GATCG	CACCAAGACCAGAGCT GTCA	246	CTA GGC CAC AGA ATT GAA AGA TCT	GTA GGT GGA AAT TCT AGC ATC ATC C	324
GCamp6	TGGGGACGGTGATGC GGTCT	ACGTGGCGAAGCTCTG CTGC	~300	CAA ATG TTG CTT GTC TGG TG	GTC AGT CGA GTG CAC AGT TT	200
M3	ACC GTC AGA TCG CCT GGA GA	TCA TCG GTG GTA CCG TCT GGA G	200	TCC TCA AAG ATG CTC ATT AG	GTA ACT CAC TCA TGC AAA GT	340

Methods

Animal protocols

All mice were kept on a 12-h light/12-h dark schedule in a humidity and temperature-controlled environment. All experiments in Norway were performed in accordance with the Norwegian Animal Welfare Act and the European Convention for the Protection of Vertebrate Animals used for Experimental and Other Scientific Purposes. All experiments involving animals in the US (pronuclear injection and husbandry of the resulting animals) were performed in accordance with guidelines approved by University of Oregon's Animal Care and Use Committee and the National Institutes of Health Guide for the Care and Use of Laboratory Animals (National Institutes of Health Publications No. 80-23).

Microdissection

Two C57black6 mice (P56) were deeply anesthetized by injection with pentobarbital (100mg/ml in 96% ethanol, Ås produksjonslab AS). The brains were removed and horizontal or coronal 500 μ m sections were cut on a Leica VT 1000 S microtome and kept at 4 °C until dissection. Bilateral dissection was performed, while watching the tissue through a dissection microscope with transmitted and reflected white light (Zeiss Discovery V8 stereomicroscope) applying architectonic criteria (Boccaro et al., 2015; Jones and Witter, 2007; O'Reilly et al., 2015; Sugar and Witter, 2016; Witter, 2011) to unstained tissue. The tissue samples were snap-frozen in liquid nitrogen, kept at -80°C and shipped on dry ice.

All dissections avoided border regions, i.e., were taken centered in the identified cortical area. In horizontal sections, MEC is easily recognized by the marked shape of the cortex, the prominent white, opaque lamina dissecans and the radial organization of the layers deep to the latter. Layer II neurons are large spherical neurons, which differ markedly in level of opacity from those in layer III. The medial border between MEC and parasubiculum is characterized by the loss of the differentiation between layers II and III, and the border with the laterally adjacent postrhinal cortex is characterized by the loss of the large spherical neurons in layer II. We only sampled the more dorsal and central portions of MEC. LEC shares the large layer II neurons with MEC, but the radial organization in layer V is absent. The anterior and dorsal border of LEC with the perirhinal cortex is characterized by the abrupt disappearance of the large layer II neurons. We only sampled the most lateral portions of LEC, as to avoid contamination with ventromedially adjacent components of the amygdaloid complex. ACC and RSC were sampled from the medial wall of the lateral hemisphere above the corpus callosum, avoiding the most anterior part of ACC and the posteroventral part of RCS. Since the border between the two areas coincides with the dorsal-anterior tip of the hippocampal formation, all samples avoided that border region.

In coronal sections, ACC and RSC samples were taken dorsal to the corpus callosum, just below the shoulder of the medial wall of the hemisphere down to, but not touching the corpus callosum, as to avoid inclusion of the indusium griseum. Samples were taken from sections anterior to the most anterodorsal tip of the hippocampal formation in case of ACC and posterior to the tip in case of RSC. Samples of LEC were collected one section after the disappearance of the piriform cortex characterized by a densely packed thick layer II, a polymorph lightly packed deeper cell layer and the presence of the endopiriform nucleus. LEC shows cytoarchitectonic features similar to those described above. We sampled only from the vertical part of LEC, directly below the rhinal fissure. For MEC, samples were collected from more posterior coronal sections, using shape of the section, the presence of the ventral hippocampus and cytoarchitectonic features as described above, as our selection criteria.

ChIP seq

All dissected brain tissues were briefly homogenized and cross-linked with 1% formaldehyde at room temperature with rotation for 15 min. Cross-linking was quenched with glycine (150mM in PBS), then tissue was washed and flash frozen. Chromatin was extracted as previously described (Cotney et al., 2013; Cotney and Noonan, 2015). Briefly, nuclei were extracted, lysed, and sonicated (30 min, 10-sec pulses) to produce sheared chromatin with an average length of ~250 bp. 1 to 10 micrograms of final soluble chromatin was used for each ChIP and combined with Protein G Dynabeads (Invitrogen, cat# 10004D) prebound with 5 µg of antibodies to H3K4me2 (Abcam ab7766) or H3K27ac (Abcam ab4729). Immunoprecipitated chromatin was washed five times with 1 mL of wash buffer and once with TE. Immunoprecipitated chromatin was eluted, cross-links were reversed, and DNA was purified. Libraries were prepared for sequencing using NEBNext ChIP-Seq Library Prep reagents and sequenced on the Illumina HiSeq 2000 platform at the Yale Center for Genome Analysis.

ChIP-seq data analysis

ChIP-Seq data was initially processed as previously described (Reilly et al 2015). Briefly, reads were aligned to the mm9 version of the mouse genome using bowtie (v1.1.1) (Langmead and Salzberg, 2012). Enriched regions were identified in individual replicates using a sliding window method as previously described (Mikkelsen et al., 2010). Enriched regions were divided into functional categories based on overlaps with genomic features as annotated by Ensembl v67 using Bedtools (2.19.0) (Quinlan and Hall, 2010). Reproducibly enriched regions were determined as the union of overlapping regions identified in both biological replicates. Putative enhancer regions from intergenic and intronic portions of the genome were then assigned target genes using GREAT. H3K27ac ChIP-Seq reads were retrieved from Encodeproject.org for 17 mouse tissues (Shen et al., 2012) and uniformly processed as above. Enhancers for all cell types were combined and merged to generate a uniform annotation of all possible enhancers. H3K27ac counts at each enhancer from each tissue were calculated using mrQuantifier (Habegger et al., 2011). Pearson correlations for all enhancer signals were calculated and plotted using R (<https://www.r-project.org/>). K-means clustering of H3K27ac count matrix was performed using Cluster (v3.0) (de Hoon et al., 2004). Rows were centered on the mean value of the row and normalized, the k parameter was the total number of tissues, and 100 runs were performed. The clustering result was then visualized using Java TreeView (Saldanha, 2004). Subregion specific clusters of enhancers were intersected with peak calls from all other tissues to identify enhancers with likely tissue specific function. Subregion specific enhancers were assigned two target genes using GREAT, ranked by H3K27ac signal, and overlapped with vertebrate conserved sequences (Siepel et al., 2005).

Cloning of transgenic constructs

The putative enhancers sequences were cloned from BACs (chori.org) and transferred to pENTRtm/D-TOPO[®] vectors by TOPO[®] cloning (Invitrogen, K2400-20). The putative enhancers were transferred to injection plasmids by gateway cloning[®] (Invitrogen, 11791-019). The resulting plasmids consist of a putative enhancer followed by a mutated heatshock promoter 68 (HSP68), a tTA gene, a synthetic intron and a WPRE element (sup. figure 3).

Pronuclear injection

The ten injection plasmids were linearized by enzyme digestion to keep the relevant elements but remove the bacterial elements of the plasmids. Linearized vectors were run on a 1% agarose gel and isolated using a Zymoclean Gel DNA Recovery Kit (Zymo research, D4001). Fertilized eggcells were injected with 1µl of DNA at concentrations of 0.5 to 1 ng/µl, leading to surviving pups of which 96 were genotypically positive for MEC and 9 were genotypically positive for LEC (sup. table 2). Pronuclear injections were done at the transgenic mouse facility of the University of Oregon

Mouse husbandry

Mouse lines were named after the ranked enhancers identified in this study, as specified in supplemental table 1. The nomenclature consists of firstly the targeted region, secondly the year of microdissection, thirdly the rank of the enhancer that corresponds with the row in supplemental table 1 and finally a letter for the founder. To illustrate, line MEC-13-53A is based on MEC tissue isolated in 2013, where the particular enhancer was ranked 53 and the founder is specified by the "A".

All genotypically positive founders based on MEC enhancers were initially mated with histone GFP mice (Jackson laboratory, Tg(tetO-HIST1H2BJ/GFP)47Efu, stocknr. 005104), while those based on LEC enhancers were mated with GCaMP6 mice (in house made). Double positive pups were used for further analysis. Subsequent crosses were done with GCaMP6 mice (in house made), TVAG mice (Line TVAG5 from (Weible et al., 2010)), ArChT mice (Weible et al., 2014), tetO-eGFP (Jackson laboratory, C57BL/6J-Tg(tetO-EGFP/Rpl10a)5aReij/J_JAX) and HM3 mice (Alexander et al., 2009).

Genotyping

Genotyping was done on ear tissue using a Kapa mouse genotyping kit (Kapa Biosystems, Cat# KK7302). Primer pairs for the appropriate gene and internal controls (supplemental table 3) are added to the PCR mixture at a final concentration of 10 μ M. The PCR reaction was done by an initial step of 4 minutes at 95 $^{\circ}$ C, then 20 cycles of 1 minute at 95 $^{\circ}$ C, 30 seconds at 70 $^{\circ}$ C reduced by 0.5 $^{\circ}$ C each cycle, and 30 seconds at 72 $^{\circ}$ C. This is followed by 20 cycles of 30 seconds at 95 $^{\circ}$ C, 30 seconds at 60 $^{\circ}$ C, and 30 seconds at 72 $^{\circ}$ C. Then a final 7 minute step at 72 $^{\circ}$ C. The products are run on a 1% agarose gel along with positive and negative controls.

In situ hybridization

Double positive mice (tTA+/-, reporter gene+/-) were deeply anesthetized with pentobarbital and transcardially perfused with 0.9% saline first and freshly made 4% formaldehyde (in 1x DPBS, thermofisher, Cat# 14200075) second. Brains were removed and postfixed overnight in 4% paraformaldehyde. Subsequently the brains were dehydrated for at least 24h with 30% sucrose in 1x PBS. The brains were sectioned sagittally at 30 μ m on a cryostat, mounted directly (on Fisherbrand Superfrost Plus microscope slides (Fisher Scientific Cat #12-550-15)) and dried overnight at room temperature. Slides were stored at -80 $^{\circ}$ C.

Slides were thawed in closed containers. Sections were outlined with a PAP pen (Sigma, cat# Z377821-1EA). The probe was diluted (usually 0.1-1 μ g/ml) in hybridisation buffer (1:10 10x salt solution, 50% deionized formamide (sigma, cat# D-4551), 10% dextran sulfate (sigma, cat# D-8906), 1mg/ml rRNA (sigma, Cat#R5636), 1x Denhardt's (Sigma cat# D-2532). Salt solution (10x) was made with 114g NaCl, 14.04g TrisHCl, 1.3g TrisBase, 7.8g NaH₂PO₄·2H₂O, 7.1g Na₂HPO₄ in H₂O to 1000ml with a final concentration of 0.5M EDTA). The probe was denatured for 10 min at 62 $^{\circ}$ C, added to the section and coverslipped (Fisher, cat# 12-548-5P). The slides were incubated overnight at 62 $^{\circ}$ C in a closed box with filter paper wetted in 1x SSC with 50% formamide.

The slides were transferred to polypropylene Coplin jars containing 1x SSC with 50% formamide and 0.1% Tween-20 warmed to 62 $^{\circ}$ C for 10 minutes to allow the coverslips to fall off. The slides were washed 3x30 minutes at 62 $^{\circ}$ C. Then the slides were washed 3x30 minutes in MABT (11.6g Maleic acid (sigma, cat#M0375-1kg), 8.76g NaCl, 5ml 20% tween, pH 7.5, ddH₂O to 1000ml) at room temperature.

The slides were drained (not dried) and re-circled with a PAP pen. Then blocking solution was added (600 μ l MABT, 200 μ l sheep serum, 200 μ l 10% blocking reagent (Roche cat#11 096 176 001)) and slides were incubated in a Perspex box with wetted filter paper at room temperature for 2-3 hours. The slides were drained and 1:5,000 sheep anti-dig AP in blocking solution was added followed by overnight incubation.

4g of polyvinyl alcohol was dissolved into 40ml AP staining buffer (100mM NaCl, 50mM MgCl₂, 100mM Tris pH9.5, 0.1% Tween-20) by heat and cooled to 37°C. The slides were washed in MABT 5 times for 4 minutes. And subsequently washed 2x10 minutes in AP staining buffer. Nitroblue tetrazolium chloride (Roche, cat# 11 383 213 001. At 3.5 µl/ml), 5-Bromo-4-chloro-3-indolyl-phosphate,4-toluidene salt (Roche, cat# 11 383 221 001. At 2.6 µl/ml) and Levamisole (Vector, cat# SP-5000. At 80µl/ml) was added to the cool polyvinyl alcohol solution. This was shaken well and transferred to a Coplin jar. The slides were added to the jar and incubated at 37°C for 3 to 5 hours. The reaction was stopped by washing in 2xPBS with 0.1% Tween-20. The slides were subsequently wash 2X in ddH₂O, and dehydrated quickly through graded ethanols from 50%, 70%, 95% to 100% ethanol. Finally the slides were cleared in xylene and coverslipped.

Immunohistochemistry

Double positive mice (tTA+/-, TVAG+/-) were deeply anesthetized with pentobarbital and transcardially perfused with approximately 30ml 0.9% saline first and approximately 30ml freshly made 4% paraformaldehyde (in 1x DPBS, thermofisher, Cat# 14200075) second. Brains were removed and postfixed for 24 hours in 4% paraformaldehyde. Subsequently the brains were dehydrated with 30% sucrose in 1x PBS. The brains were sectioned horizontally at 50µm and kept in TCS (tissue collection solution, 25% glycerol, 35% ethyl glycol, 50% 1xDPBS) at -20°C.

Immunohistochemistry was done by two initial 10 minute washes in 1xDPBS and subsequent permeabilized by a 60 minute wash in 1% Triton X-100 (Sigma, Cat#T9284) in 1xDPBS. Then the tissue is incubated in primary antibody in 1xDPBS with 1% triton X-100 and 5% donkey serum (Sigma, Cat# D9663) for 48 hours at 4°C. Primary antibodies and dilutions were: Rabbit-anti-2A (1:2000, Millipore, cat#ABS31), Mouse-anti-reelin (1:1000, Millipore, cat# Mab5364), Mouse-anti-GAD67 (1:1000, Millipore, cat# Mab5406), Mouse-anti-calbindin (1:10000, Swant, cat# CB300).

After incubation with primary antibodies, sections were washed 4x in 1xDPBS (10 minutes per wash) and 2x in 1xDPBS with 1% Triton X-100. Then sections were incubated for 6h at room temperature in secondary antibody (all secondary antibodies were raised in Donkey and diluted 1:250). The secondary antibodies were: anti-Rabbit-AF488 (Jackson ImmunoResearch, Cat# 711-545-152) and anti-Mouse-Cytm3 (Jackson ImmunoResearch, Cat# 715-165-151)

The sections were DAPI stained by a single 10 minute wash in 1xDPBS with 0.2µg/ml DAPI (thermofisher, D1306) and finally washed 5x (10 minutes per wash) in 1x DPBS. Sections were mounted on superfrost[®] plus glass slides (VWR, Cat# 631-9483) and coverslipped with polyvinyl alcohol with 2.5% DABCO (Sigma, Cat# D27802).

Imaging

From mice in the lines MEC-13-53A x TVAG and MEC-13-104B x tetO-eGFP MEC was imaged on sections from three different dorsal-ventral levels with a Zeiss Meta 880 confocal microscope. For each section, three to seven slices in the Z direction with 1.5µm spacing were taken, with a 20x objective and tiling to cover the entire MEC. Two channels were imaged, one for AF488 with maximum excitation wavelength at 488nm and maximum emission wavelength at 528nm and one for Cy3 with maximum excitation wavelength at 561nm and maximum emission wavelength at 595nm.

For display images, sections were imaged on Zeiss Axio.scan Z1 scanners in three preset channels: DAPI, dl488 and dl549.

Image processing

From the Zeiss proprietary file format .lsm, .tiff files were exported. These were processed in Adobe Photoshop, all alterations in levels were made on the entire images. In some cases images were processed to remove visual artifacts and background.

Counting

Counts were made on the confocal images for single positive cells expressing transgenes, cells expressing native genes (GAD67, Reelin, Calbindin) and cells expressing both. Graphs were made in Microsoft excel, statistical analysis was done in SPSS.

- Alexander, G.M., Rogan, S.C., Abbas, A.I., Armbruster, B.N., Pei, Y., Allen, J.A., Nonneman, R.J., Hartmann, J., Moy, S.S., Nicolelis, M.A., *et al.* (2009). Remote control of neuronal activity in transgenic mice expressing evolved G protein-coupled receptors. *Neuron* *63*, 27-39.
- Boccarda, C.N., Kjonigsen, L.J., Hammer, I.M., Bjaalie, J.G., Leergaard, T.B., and Witter, M.P. (2015). A three-plane architectonic atlas of the rat hippocampal region. *Hippocampus* *25*, 838-857.
- Cotney, J., Leng, J., Yin, J., Reilly, S.K., DeMare, L.E., Emera, D., Ayoub, A.E., Rakic, P., and Noonan, J.P. (2013). The evolution of lineage-specific regulatory activities in the human embryonic limb. *Cell* *154*, 185-196.
- Cotney, J.L., and Noonan, J.P. (2015). Chromatin immunoprecipitation with fixed animal tissues and preparation for high-throughput sequencing. *Cold Spring Harb Protoc* *2015*, 419.
- de Hoon, M.J., Imoto, S., Nolan, J., and Miyano, S. (2004). Open source clustering software. *Bioinformatics* *20*, 1453-1454.
- Habegger, L., Sboner, A., Gianoulis, T.A., Rozowsky, J., Agarwal, A., Snyder, M., and Gerstein, M. (2011). RSEQtools: a modular framework to analyze RNA-Seq data using compact, anonymized data summaries. *Bioinformatics* *27*, 281-283.
- Jones, B.F., and Witter, M.P. (2007). Cingulate cortex projections to the parahippocampal region and hippocampal formation in the rat. *Hippocampus* *17*, 957-976.
- Langmead, B., and Salzberg, S.L. (2012). Fast gapped-read alignment with Bowtie 2. *Nature methods* *9*, 357-359.
- Mikkelsen, T.S., Xu, Z., Zhang, X., Wang, L., Gimble, J.M., Lander, E.S., and Rosen, E.D. (2010). Comparative epigenomic analysis of murine and human adipogenesis. *Cell* *143*, 156-169.
- O'Reilly, K.C., Flatberg, A., Islam, S., Olsen, L.C., Kruge, I.U., and Witter, M.P. (2015). Identification of dorsal-ventral hippocampal differentiation in neonatal rats. *Brain Struct Funct* *220*, 2873-2893.
- Quinlan, A.R., and Hall, I.M. (2010). BEDTools: a flexible suite of utilities for comparing genomic features. *Bioinformatics* *26*, 841-842.
- Saldanha, A.J. (2004). Java Treeview--extensible visualization of microarray data. *Bioinformatics* *20*, 3246-3248.
- Shen, Y., Yue, F., McCleary, D.F., Ye, Z., Edsall, L., Kuan, S., Wagner, U., Dixon, J., Lee, L., Lobanenkov, V.V., *et al.* (2012). A map of the cis-regulatory sequences in the mouse genome. *Nature* *488*, 116-120.
- Siepel, A., Bejerano, G., Pedersen, J.S., Hinrichs, A.S., Hou, M., Rosenbloom, K., Clawson, H., Spieth, J., Hillier, L.W., Richards, S., *et al.* (2005). Evolutionarily conserved elements in vertebrate, insect, worm, and yeast genomes. *Genome research* *15*, 1034-1050.
- Sugar, J., and Witter, M.P. (2016). Postnatal development of retrosplenial projections to the parahippocampal region of the rat. *Elife* *5*.
- Weible, A.P., Moore, A.K., Liu, C., DeBlander, L., Wu, H., Kentros, C., and Wehr, M. (2014). Perceptual gap detection is mediated by gap termination responses in auditory cortex. *Current biology : CB* *24*, 1447-1455.
- Weible, A.P., Schwarcz, L., Wickersham, I.R., DeBlander, L., Wu, H., Callaway, E.M., Seung, H.S., and Kentros, C.G. (2010). Transgenic targeting of recombinant rabies virus reveals monosynaptic connectivity of specific neurons. *The Journal of neuroscience : the official journal of the Society for Neuroscience* *30*, 16509-16513.
- Witter, M.P. (2011). The hippocampus. In *The Mouse Nervous System*, G. Paxinos, L. Puelles, and C. Watson, eds. (Academic Press), pp. pp 112-139.